Published in final edited form as:
Mol Pharm. 2013 February 4; 10(2): 739–755. doi:10.1021/mp300563m.

Metal-Catalyzed Oxidation of Protein Methionine Residues in Human Parathyroid Hormone (1-34): Formation of Homocysteine and a Novel Methionine-Dependent Hydrolysis Reaction

Olivier Mozziconacci[†], **Junyan A. Ji**[‡], **Y. John Wang**[‡], and **Christian Schöneich**[*,†]

[†]Department of Pharmaceutical Chemistry, 2095 Constant Avenue, University of Kansas, Lawrence, Kansas 66047, United States

[‡]Late Stage Pharmaceutical Development Department, Genentech, South San Francisco, California 94080, United States

Abstract

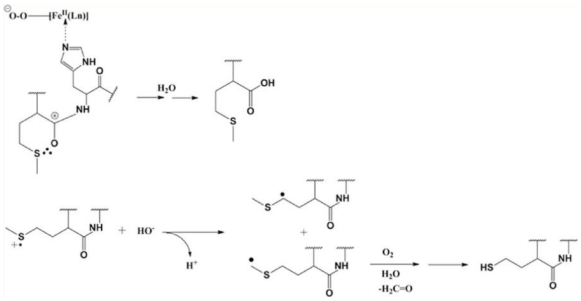

The oxidation of PTH(1-34) catalyzed by ferrous ethylenediaminetetraacetic acid (EDTA) is site-specific. The oxidation of PTH(1-34) is localized primarily to the residues Met[8] and His[9]. Beyond the transformation of Met[8] and His[9] into methionine sulfoxide and 2-oxo-histidine, respectively, we observed a hydrolytic cleavage between Met[8] and His[9]. This hydrolysis requires the presence of Fe^{II} and oxygen and can be prevented by diethylenetriaminepentaacetic acid (DTPA) and phosphate buffer. Conditions leading to this site-specific hydrolysis also promote the transformation of Met[8] into homocysteine, indicating that the hydrolysis and transformation of homocysteine may proceed through a common intermediate.

Keywords

parathyroid hormone; alanine; methionine; homocysteine; methionine radical cation; Fenton reaction; hydrolysis; mass spectrometry

[*]**Corresponding Author** Department of Pharmaceutical Chemistry, 2095 Constant Avenue, University of Kansas, Lawrence, Kansas 66047, United States. schoneic@ku.edu. Phone: (785) 864 4880. Fax: (785) 864 5736..

Supporting Information

Figure S1–S10. This material is available free of charge via the Internet at http://pubs.acs.org.

The authors declare no competing financial interest.

1. INTRODUCTION

Protein oxidation is frequently observed in biological aging[1–3] and represents a common problem limiting the stability of protein formulations.[4] Frequently, the mechanisms leading to protein oxidation in pharmaceutical formulations are not well understood due to the manifold of possible reactions and the potential for varying degrees of protein and/or excipient impurities to influence reactions pathways. Specific oxidants can react selectively with individual amino acids and form specific oxidation products depending on the reaction conditions (i.e., the nature of the formulation). A classic example is the reaction of hydrogen peroxide, which predominantly oxidizes Met to Met sulfoxide;[5–8] however, in the presence of transition metals, hydrogen peroxide can be converted to hydroxyl radicals through the Fenton reaction.[9] In contrast to hydrogen peroxide, hydroxyl radicals react with all amino acids.[10] Frequently, protein formulations are contaminated by transition metals introduced through buffers, protein, and excipients or leaching from the metal container. When proteins contain binding sites for such transition metals, transition metal-catalyzed oxidation reactions can occur site-specifically, where the respective target sites for oxidation on a protein are defined by the location of the metal-binding sites. An important example is the oxidation of His residues and/or amino acids (e.g., Met) in close vicinity to His residues, which constitute binding sites for transition metals.[11–13] Here, the binding of the catalytic metal to His directs the oxidation toward amino acid targets in protein domains, which would not necessarily be targeted for oxidation based on solvent-accessible surface area. For example, the metal-catalyzed oxidation of human relaxin resulted in the oxidation of His and Met.[14] Among two Met residues, Met(B4) was oxidized to a higher extent than Met(B25), rationalized by the presence of metal-binding residues in the vicinity of Met(B4). In contrast, the exposure to human relaxin to hydrogen peroxide alone resulted in the opposite preference, a higher oxidation sensitivity of Met(B25). It was also demonstrated that, during the preparation of a recombinant humanized monoclonal antibody fragment in the presence of polysorbate 20, metal-binding to His[31] (in the Fab region) mediated the oxidation of Trp[50].[15]

The mechanisms of metal-catalyzed oxidation are complex, involving a manifold of potential short-lived intermediates such as freely diffusible and/or metal-bound hydroxyl radicals as well as metal-bound peroxides. Importantly, the extent to which these intermediates may be responsible for protein oxidation may vary from protein to protein based on protein conformation and the geometries of the metal-binding sites. In addition, the nature of the redox-active metal will define the actual oxidation mechanism. Based on product and kinetic isotope effects, the metal-catalyzed oxidation of human growth hormone by Cu^{II}/ascorbate likely involves hydroxyl radicals ($HO^{\bullet}$).[12] In contrast, scavenger studies during the oxidation of small Met-containing peptides by the classic Fenton system, $[Fe^{II}(EDTA)]^{2-}/H_2O_2$, are more consistent with a “complexed” or metal-bound hydroxyl radical.[16]

2. MATERIALS AND METHODS

2.1. Materials

Human parathyroid hormone (1-34) (PTH(1-34)) (SVSEIQLMHNLGKHLNSMERVEWLRKKLQDVHNF, mol wt: 4117.72 Da, Figure 1) was supplied by American Peptide Co. Inc. (Sunnyvale, CA, USA). The PTH(1-34) Met[8]Ala mutant was synthesized at Genentech (South San Francisco, CA, USA). Ammonium acetate (AAc), sodium phosphate (NaH_2PO_4), iron(II) sulfate heptahydrate ($FeSO_4 \times 7H_2O$), iron(III) sulfate hydrate ($Fe_2(SO_4)_3 \times H_2O$), ethylenediaminetetraacetic acid (EDTA), diethylenetriaminepentaacetic acid (DTPA), *N*-ethylmaleimide (NEM), and catalase from bovine liver were supplied by Sigma-Aldrich (St. Louis, MO, USA) at the

highest purity grade. Hydrogen peroxide (H_2O_2, 30%) was supplied by Fisher Scientific (Pittsburgh, PA, USA). Sequencing trypsin grade was supplied by Promega (Madison, WI, USA). To ensure that our solutions were not contaminated by any protease, some control experiments were performed according to the experimental protocols 1 and 5 (see below Section 2.3) in the presence of protease inhibitors (cOmplete ULTRA Tablets, Roche, Indianapolis, IN, USA). In addition, to probe for potential bacterial contamination, a series of control experiments was performed with solutions which had been subjected to sterile filtration, using a sterile syringe filter equipped with a 0.2 μm membrane (Corning Incorporated, New York, NY, USA) and used in a sterile room.

2.2. Digestion of PTH(1-34) and PTH(1-34) Met[8]Ala

PTH(1-34) and PTH(1-34) Met[8]Ala were digested with trypsin (1 μg/mL) in ammonium bicarbonate buffer (50 mM, pH 8.0) at 37 °C for 3 h. The digestion was either performed under air or Ar. This experimental parameter is given in Section 2.3 along with the description of the different protocols for the oxidation of PTH(1-34) and its mutant.

The proteolytic cleavage sites are presented in Figure 1. Fragments **F1–F4** indicate the location of tryptic peptides shared by PTH(1-34) and PTH(1-34) Met[8]Ala, which are rather insensitive to chemical modification by the Fenton reaction. Fragments **F5** and **F5A** indicate the location of the N-terminal tryptic fragments of PTH(1-34) and PTH(1-34) Met[8]Ala, respectively, which are the predominant target sites for modification by the Fenton reaction. Although PTH is not very hydrophobic and could have been analyzed as an intact protein by high-performance liquid chromatography, we preferred to tryptic digest PTH. The possible formation of cross-links during the metal-catalyzed oxidation of PTH may generate high molecular weight products. Indeed, the oxidation of Tyr and Phe residues can mediate the formation of cross-links with amino groups through Michael addition.[17]

2.3. Oxidation of PTH(1-34) by the Fenton Reaction

PTH(1-34) was oxidized according to different protocols, referred to as Exp.1–Exp.10, schematically displayed in Figure 2. The stock solutions of Fe^{II}/EDTA, Fe^{II}/DTPA, and H_2O_2 were prepared at a concentration of 10 mM in ammonium acetate buffer (20 mM, pH 6.9). The stock solution of DTPA was prepared at a concentration of 1 mM in ammonium acetate buffer (20 mM, pH 6.9). PTH(1-34) and catalase were prepared at a concentration of 24.3 μM (0.1 mg/mL) and 1.4 μM, respectively, in ammonium acetate buffer (20 mM, pH 6.9). The stock solutions of Fe^{II}/EDTA, Fe^{II}/DTPA, H_2O_2, and PTH(1-34) were always prepared and kept under Ar. Subsequently, the incubation of the reaction mixtures was performed either under air (Exp. 1–4 and 8) or under Ar (Exp. 5–7). After 15 min reaction time, 25 μL of catalase (1.4 μM) were added to the final solution to remove H_2O_2. When applicable, digestions were performed in the presence of air, according to the protocol described in Section 2.2.

2.3.1. Protocol Exp. 1 (Figure 2a)—Samples of 10 μL each of Fe^{II}/EDTA and H_2O_2 were mixed under Ar with 980 μL of PTH(1-34) to yield initial molar ratios of $[Fe^{II}(EDTA)]^{2-}/H_2O_2/$ PTH(1-34) = 1:1:0.24 (it is important to note that not all oxidants generated through reactions 1–4 will be available to react with PTH(1-34) as these oxidants also readily react with $[Fe^{II}(EDTA)]^{2-}$).[18] The reaction vial was opened to air, and after 30 min of incubation at 37 °C under air, 250 μL of the reaction sample were diluted with 250 μL of DTPA (1 mM) (the use of DTPA serves to terminate a hydrolysis reaction which will be confirmed in Exp. 2 below). Digestion was performed according to the protocol given in Section 2.2.

2.3.2. Protocol Exp. 2 (Figure 2a)—Sample of 10 μL each of Fe^{II}/DTPA and H_2O_2 were mixed with 980 μL of PTH(1-34). After 30 min of incubation at 37 °C under air, 250 μL of the reaction sample was diluted with 250 μL of DTPA (1 mM). Digestion was performed according to the protocol given in Section 2.2.

2.3.3. Protocol Exp. 3 (Figure 2a)—Samples of 10 μL each of Fe^{II}/EDTA and H_2O_2 were mixed under Ar with 980 μL of PTH(1-34). After 30 min of incubation at 37 °C under air, 250 μL of the reaction sample was diluted with 250 μL of ammonium acetate buffer (20 mM, pH 6.9). In contrast to the protocols of Exp. 1 and Exp. 2, the hydrolysis reaction was not terminated through the addition of DTPA.

2.3.4. Protocol Exp. 4 (Figure 2a)—Samples of 10 μL each of Fe^{II}/EDTA and 10 μL of water were mixed with 980 μL of PTH(1-34). In contrast to Exp. 1 and 2, no H_2O_2 was added to the reaction sample. After 30 min of incubation at 37 °C under air, 250 μL of the reaction sample was diluted with 250 μL of DTPA (1 mM). Digestion was performed according to the protocol given in Section 2.2.

2.3.5. Protocol Exp. 5 (Figure 2b)—Samples of 10 μL each of Fe^{II}/EDTA and H_2O_2 were mixed with 980 μL of PTH(1-34). After 30 min of incubation at 37 °C under Ar, 250 μL of the reaction sample was mixed, under Ar, with 250 μL of ammonium acetate buffer (20 mM, pH 6.9). The reaction was also run at pH 7.9 and 4.5. The pH of the buffers was adjusted to the new values by using 1 M NaOH or 1 M HCl. Digestion was performed according to the protocol given in Section 2.2.

2.3.6. Protocol Exp. 6 (Figure 2b)—Samples of μL each of Fe^{II}/EDTA and H_2O_2 were mixed with 980 μL of PTH(1-34). After 30 min of incubation at 37 °C under Ar, 250 μL of the sample was combined with 250 μL of DTPA (1 mM) under Ar. After 15 min, 25 μL of catalase (1.4 μM) was added to the final solution (kept under Ar) prior to digestion. The digestion was performed under Ar according to the protocol described in Section 2.2.

2.3.7. Protocol Exp. 7: Oxidation in the Absence of Metal—Samples of 10 μL each of DTPA and H_2O_2 were mixed with 980 μL of PTH(1-34). After 30 min of incubation at 37 °C under Ar, 25 μL of catalase (1.4 μM) were added to the final solution (kept under Ar) prior to digestion. The digestion was performed under Ar according to the protocol described in Section 2.2.

2.3.8. Protocol Exp. 8: Replacement of $[Fe^{II}(EDTA)]^{2-}$ by $[Fe^{III}(EDTA)]^{-}$—Samples of 10 μL each of Fe^{III}/EDTA and H_2O_2 were mixed with 980 μL of PTH(1-34). After 30 min of incubation at 37 °C under Ar, 25 μL of catalase (1.4 μM) were added to the final solution (kept under Ar) prior to digestion. The digestion was performed under Ar according to the protocol described in Section 2.2.

2.3.9. Protocol Exp. 9: Oxidation in the Presence of Fe^{II} and Absence of EDTA and H_2O_2—A $FeCl_2$ stock solution (10 mM) was prepared in ammonium acetate buffer (pH 6.9). The buffer was Ar-saturated before the addition of Fe^{II}. A sample of 10 μL of this solution was mixed with 990 μL of PTH(1-34). After 30 min of incubation at 37 °C under Ar, the solution was opened to air. No catalase was added to the final solution prior to digestion. The digestion was performed under air.

2.3.10. Protocol Exp. 10: Oxidation in the Presence of H_2O^{18}—For this experimental protocol, 10 μL each of Fe^{II}/EDTA and H_2O_2 of which the stock solutions were prepared in H_2O^{16}, were mixed with 980 μL of PTH(1-34) prepared in H_2O^{18}. After

30 min of incubation at 37 °C under air, 250 μL of the reaction sample were diluted with 250 μL of DTPA (1 mM). After 15 min, 25 μL of catalase (1.4 μM) were added to the final solution. This sample was not digested.

2.3.11. Detection of Homocysteine—PTH(1-34) was oxidized according to the experimental protocols Exp. 1 (Section 2.3.1) and Exp. 9 (Section 2.3.9). After oxidation, NEM (1 mM) was added to the sample. The pH of the solution was adjusted to 8.0 by the addition of NaOH. After incubation at 37 °C for 30 min, β-mercaptoethanol (10 mM) was added to the solution prior to the start of the digestion. The digestion was performed according to the protocol described in Section 2.1. NEM served to alkylate the thiol group of the homocysteine residue.

2.4. Sample Preparation for Capillary LC-MS Analysis

LC-MS analyses of the reaction mixtures (prepared according to the protocols Exp.1–10) were performed on a Capillary Liquid Chromatography System (Waters Corporation, Milford, MA, USA). Samples of 10 μL of each sample were injected onto a C18 Vydac column (25 cm × 0.5 mm, 3.5 μm) and eluted with a linear gradient delivered at the rate of 20 μL/min. Mobile phases consisted of water/acetonitrile/formic acid at a ratio of 99%, 1%, and 0.08% (v:v:v) for solvent A and a ratio of 1%, 99%, and 0.06% (v:v:v) for solvent B. The following linear gradient was set: 10–50% of solvent B within 30 min.

2.5. Nano-Electrospray Ionization Time-of-Flight MS (ESI-TOF-MS) Analysis

ESI-MS spectra of undigested PTH(1-34) and of the peptide digests were acquired on a SYNAPT-G2 (Waters Corp., Milford, MA). The SYNAPT-G2 instrument was operated for maximum resolution with all lenses optimized on the $[M + 2H]^{2+}$ ion from the $[Glu]^1$-fibrinopeptide B. The cone voltage was 45 V, and Ar was admitted to the collision cell. The spectra were acquired using a mass range of 50–2000 amu (= atomic mass unit). The data were accumulated for 0.7 s per cycle.

2.6. MS/MS Analysis

The proteolytic digest of PTH(1-34) was analyzed either by means of a SYNAPT-G2 (Waters Corp., Milford, MA, USA) or an LTQ-FT mass spectrometer (Thermo Finnigan, West Palm Beach, FL, USA) under conditions described elsewhere. [19] On the SYNAPT-G2, MS/MS spectra were acquired by setting the MS^1 quadrupole to transmit a precursor mass window of ±0.1 amu. The MS/MS spectra were analyzed with the software MassMatrix[20–23] and ProteinLynx Global Server from Waters Corp. (Milford, MA, USA). On the LTQ-FT mass spectrometer, peptides were separated on a reverse-phase LC Packings PepMap C18 column (0.300 × 150 mm) at a flow rate of 10 μL/min with a linear gradient rising from 0 to 65% acetonitrile in 0.06% aqueous formic acid over a period of 55 min using LC Packing Ultimate Chromatograph (Dionex). LC-MS experiments were performed in a data-dependent acquisition manner using the Xcalibur 2.0 software (Thermo Scientific West Palm Beach, FL, USA). The five most intensive precursor ions in a survey MS^1 mass spectrum acquired in the Fourier transform-ion cyclotron resonance over a mass range of 300–2000 *m/z* were selected and fragmented in the linear ion trap by collision-induced dissociation. The ion selection threshold was 500 counts. For both instruments, the theoretical fragments were compared to the experimental MS/MS spectra to validate the structures of the products. The structures were validated only if the differences between the theoretical and the experimental *m/z* of the parent ion (and the fragment ions) were strictly below 0.1 Da.

3. RESULTS

The MS/MS spectra of the unmodified tryptic fragments of a PTH(1-34) control are presented in Figure S1–S5 (Supporting Information). The experimental protocols (Exp. 1–10) are summarized in Figure 2. A list of the sequences of the tryptic fragments of PTH(1-34), PTH(1-34) Met[8]Ala) and of some oxidation products are presented in Table 1. The results are succinctly summarized in Table 2. The relative quantification of the oxidation products was obtained by (i) calculation of the peak area for each product from the LC-MS chromatograms (total ion counts, TIC) and (ii) the calculation of the ratio: area of the peak of interest/sum of the peak areas.

3.1. Nature of Oxidation Products of PTH(1-34)

Prior to the complete description of the LC-MS chromatograms obtained after oxidation of PTH(1-34), we shall present here an overview over the different products of oxidation.

The Fenton oxidation of PTH(1-34) under air and Ar leads to the formation of three major products, **P1, P2**, and **P3** (Table 1). These products are fully characterized by their CID spectra presented in Figures 4, 5, and S6.

Product P1—P1 (*m/z* 1471.2) is the result of the oxidation of Met[8] to Met sulfoxide (MetSO). Formation of MetSO at position 8 is confirmed by MS/MS sequencing of **P1** (Figure 4). The y and b fragment ions fully characterize the sequence. In particular, the y5 (*m/z* 568.3) and y6 (*m/z* 615.4) fragments demonstrate the addition of +16 Da on Met[8] (Figure 4), and the peaks with *m/z* 651.36 and *m/z* 764.45 are derived from the neutral loss of 64 Da (CH_3SOH) from y6 and y7, respectively. The neutral loss of CH_3SOH is also observed for y8 (*m/z* 892.5) and y9 (*m/z* 1005.59).

Product P2—P2 (*m/z* 906.4) results from the hydrolysis of the peptide bond between residues Met[8] and His[9] (Table 1). The MS/MS sequencing of **P2** is presented in Figure 5. The presence of the y1 fragment ion clearly demonstrates that Met[8] represents the C-terminal residue of **P2**.

Product P3—P3 (*m/z* 1487.3) is the result of the oxidation of the residues Met[8] and His[9] to MetSO and 2-oxo-histidine,[24] respectively (Table 1). The MS/MS sequencing of **P3** is presented in the Supporting Information (Figure S6). The fragment ions y4 (*m/z* 431.3) and y6 (*m/z* 731.4) and the presence of b8 (*m/z* 904.4) demonstrate the incorporation of one oxygen into each residue, Met[8] and His[9]. The oxidation of PTH(1-34) by H_2O_2 under air leads to the formation of two major products, **P1** and **P3**. Product **P1** has been described above.

Product P4—In product **P4**, Met[8] is replaced by homocysteine. The characterization and mechanism of formation of **P4** is described in more detail below (Section 3.12).

Because products **P1, P2**, and **P3** are related to the oxidation of the residues Met[8] or Met[8] and His[9], which belong to the tryptic fragment **F5**, the yield of these products will be given throughout this paper as the relative ratio of conversion of **F5** into its respective products of oxidation, **P1, P2**, or **P3**.

Oxidation products of Met[18], Trp[23], and His[32] only formed at trace levels during the Fenton oxidation of PTH(1-34).

3.2. Fenton Oxidation of PTH(1-34) under Air: Exp. 1–4

I. Oxidation in the Presence of Fe^{II}/EDTA. In the Presence of H_2O_2 (Exp. 1 and 3)—The oxidation of PTH(1-34) by Fe^{II}/EDTA and H_2O_2 (Exp. 1 and 3, Figure 2) shows the same LC-MS profile (Figure 6B,D) independent of the addition of DTPA prior to the addition of catalase. Oxidation of PTH(1-34) under such conditions results in the formation of **P1** and **P2** (monitored after proteolytic digestion). In fact, the ratios of **P1/F5** and **P2/F5** are equal to 82% and 12% without the addition of DTPA and 83% and 11% with the addition of DTPA (Figure 3). Under these experimental conditions, the addition of DTPA after 30 min reaction time had no effect on the product yields of **P1** and **P2** since both reactions were complete prior to the addition of DTPA. As the samples were exposed to air prior to the addition of DTPA, the formation of **P2** likely occurred during air-exposure (see also below). Product **P2** was also observed by MS analysis when PTH(1-34) was not digested after Fenton oxidation. This demonstrates that the hydrolytic cleavage observed between Met[8] and His[9] did not occur during proteolytic digestion.

In the Absence of H_2O_2 (Exp. 4)—The exposure of PTH(1-34) to Fe^{II}/EDTA in the absence of H_2O_2 led to a significant decrease of the yield of **P1**, while the yield of product **P2** shows a significant increase (Figure 3; Figure 6B vs E). In the absence of H_2O_2, only 4% of Met[8] was oxidized to MetSO, as characterized by the ratio **P1/F5** (Figure 3, Exp. 4). In contrast, the ratio **P2/ F5** reached 33% (Figure 3, Exp. 4), indicating that higher yields of **P2** was formed in the absence of H_2O_2.

Oxidation Using Fe^{II}/DTPA (Exp. 2)—The LC-MS profile of the oxidation of PTH(1-34) by Fe^{II}/DTPA in the presence of H_2O_2 (Exp. 2, Figure 2) reveals only the formation of **P1** (Figure 6C), while product **P2** is not formed. The ratio **P1/F5** reached 23% under these conditions (Figure 3). We can conclude that the addition of DTPA prevented the formation of **P2** and decreased the yield of oxidation of Met[8], that is, the conversion of **F5** into **P1**.

3.3. Oxidation of PTH(1-34) under Ar: Exp. 5 and 6

PTH(1-34) was oxidized in the presence of Fe^{II}/EDTA and H_2O_2. All of the samples were maintained under Ar, from the preparation of the stock solutions until the end of the proteolytic digestion.

In the Absence of DTPA (Exp. 5)—After oxidation of PTH(1-34), no DTPA was added to the solution prior to digestion, and the reaction mixture was exposed to air only prior to LC-MS analysis (Figure 2). LC-MS analysis shows the formation of products **P1** and **P2** with a relative yield of 12% (**P1/F5**) and 34% (**P2/F5**), respectively (Figure 7A and Figure 3).

Variation of the pH (Exp. 5)—The pH was changed to 7.9 and 4.5 by the addition of NaOH or HCl, respectively, to the solution. At pH 7.9, no significant changes were observed compared to pH 6.9. Under acidic condition, pH 4.5, product **P2** was not observed. The yield **P1/F5** was 100% (Figure S7).

In the Presence of DTPA (Exp. 6)—Immediately after the oxidation of PTH(1-34), DTPA was added to the solution while still under Ar. The comparison of the LC-MS data (Figure 7A and B) demonstrates that the hydrolytic cleavage leading to the formation of **P2** does not occur during LC-MS analysis. After proteolytic digestion, LC-MS analysis revealed only the formation of product **P1** with a relative yield (**P1/F5**) of 10% (Figure 7B and Figure 3).

The data demonstrate that the formation of **P2** requires O_2 (Exp. 1 vs 5) and Fe^{II}/EDTA (Exp. 1 vs 2) but does not require H_2O_2 (Exp. 4) and can be prevented by DTPA (Exp. 4 vs 3). The two experiments described above (Section 3.3) vary only in the addition of DTPA prior to digestion (under air). It appears that, even after 30 min reaction time under Ar, some $[Fe^{II}/EDTA]^{2-}$ is left in the solution, which upon exposure to air (for digestion) promotes the hydrolysis between Met[8] and His[9]. To convert residual $[Fe^{II}/EDTA]^{2-}$ to some $[Fe^{III}/EDTA]^{-}$ under Ar, we first incubated PTH(1-34) according to experimental protocol Exp. 5 and subsequently added an excess of H_2O_2 (50 mM) under Ar, prior to exposing the solution to air. No DTPA was added. LC-MS analysis reveals that under these conditions the tryptic peptide **F5** was completely converted into **P1**. Product **P2** was not observed (Figure 8A; control, Figure 8B, is displayed to localize the peak corresponding to **F5**). The result of this experiment supports the observations emphasized in Exp. 1 vs 5 and Exp. 1 vs 2 that the formation of **P2** requires the presence of molecular oxygen and Fe^{II}. Hence, EDTA is not necessary for the formation of **P2** (see Section 3.7).

3.4. Oxidation of PTH(1-34) in the Presence of DTPA and H_2O_2 but Absence of Fe^{II}

PTH(1-34) was oxidized according to the protocol Exp. 7. The LC-MS analysis presented in Figure 9 shows that the tryptic fragment **F5** was completely transformed into product **P1**. Under these conditions of oxidation, 100% of Met[8] was therefore converted into MetSO. Product **P2** was not formed.

3.5. Oxidation of PTH(1-34) Using Fe^{III}

Following the experimental protocol Exp. 8, product **P2** was not formed if PTH(1-34) was incubated at 37 °C for 30 min in the presence of $[Fe^{III}/EDTA]^{-}$ and H_2O_2, either under Ar or air (LC-MS analysis was similar to the one obtained after oxidation of PTH(1-34) in phosphate buffer, see Figure S8A). Product **P1** was formed. The relative yield of conversion **P1/F5** was 13%.

3.6. Oxidation of PTH(1-34) in Phosphate Buffer

The experimental protocol Exp. 1 (Section 2.3.1) was modified to replace ammonium acetate buffer with potassium phosphate buffer. In potassium phosphate buffer, the oxidation of PTH(1-34) in the presence of Fe^{II}/EDTA and H_2O_2 did not yield **P2** (Figure S8A). Product **P1** was observed with a relative yield **P1/F5** = 12%.

3.7. Oxidation of PTH(1-34) Using Fe^{II} without EDTA and H_2O_2

PTH(1-34) was oxidized according to the experimental protocol Exp. 9. After incubation of PTH(1-34) in the presence of only Fe^{II} in Ar at 37 °C, the solution was exposed to air. After digestion, LC-MS analysis revealed the formation of **P2** with a relative yield **P2/F5** = 13%. **P1** was observed with a relative yield **P1/F5** = 5% (Figure S9).

3.8. Oxidation of PTH(1-34) in the Presence of Added Methionine

PTH(1-34) was oxidized according to the protocol of Exp. 1 (Section 2.3.1), except that methionine (1 mM) was added to the solution prior to incubation. The exogenous methionine prevented the formation of **P2** (relative yield **P2/F5** < 0.5%).

3.9. Preoxidation of PTH(1-34) by H_2O_2, Followed by Fenton Oxidation

PTH(1-34) was preoxidized with H_2O_2 under air prior to Fenton oxidation according to the experimental protocol Exp. 1. A representative LC-MS analysis of such preoxidized PTH(1-34) is presented in Figure 10. After proteolytic digestion, in addition to the unmodified tryptic fragments (**F2–F4**), LC-MS analysis reveals the presence of products **P1**

and **P3** (Table 1). The absence of the tryptic fragment **F5** demonstrates the conversion of Met[8] and His[9] into MetSO (**P1**) and 2-oxo-His (**P3**). The ratio **P3/P1** = 50% indicates that 66% of **F5** is converted into **P1** (ratio **P1/F5**) and 33% into **P3** (ratio **P3/F5**) (considering that the total amount of **F5** is converted into **P1** and **P3, F5** = **P1** + **P3**). After Fenton oxidation, no significant other products are observed. In particular, the absence of **P2** suggests that neither **P1** nor **P3** is a suitable precursor for **P2**.

3.10. Oxidation of PTH(1-34) Met[8]Ala under Air

PTH(1-34) Met[8]Ala was oxidized according to the experimental protocol Exp. 1 (Section 2.3.1). A comparison of nonoxidized (control) and oxidized PTH(1-34) Met[8]Ala (Figure 11) does not show any significant difference. Hence, the substitution of Met[8] by Ala[8] prevented the hydrolysis of the peptide bond between Ala[8] and His[9]. If the hydrolysis between Ala[8] and His[9] had occurred, we would have expected to observe the formation of product **P2A** (*m/z* 846.4, Table 1). The absence of **P2A** during the Fenton oxidation of PTH(1-34) Met[8]Ala demonstrates the involvement of Met[8] in the hydrolysis mechanism during the Fenton oxidation of PTH(1-34).

3.11. Oxidation of PTH(1-34) in H_2O^{18}

A mass spectrometry analysis in the range of *m/z* 906.0–912.0 (Figure 12) reveals that after Fenton oxidation of PTH(1-34) (protocol Exp. 10) in the presence of H_2O^{18}/H_2O^{16} (80:20, v:v) the ions with *m/z* 908.4 and *m/z* 906.4 are present in a 100:83 ratio; that is, close to the isotopic ratio of O^{18}/O^{16} in water under these conditions. This result demonstrates a nucleophilic attack of H_2O on an intermediate leading to the hydrolysis product.

3.12. Conversion of Met[8] into Homocysteine

During the Fenton oxidation of PTH(1-34), in the presence of $[Fe^{II}/EDTA]^{2-}$ and H_2O_2, we observed the transformation of Met[8] into homocysteine. The homocysteine residue was fully characterized by the MS/MS analysis of product **P4** (Figure 13) and **P4-NEM** (Figure 14), generated by alkylation of **P4** with NEM. The structure of **P4** is characterized by the presence of the a7, b8, y5, and y6 fragment ions, which demonstrate the loss of 14 Da from the Met[8] residue originally present in the tryptic fragment **F5** (Figure 13). **P4-NEM** contains two NEM groups located at the homocysteine and at C-terminal Lys residues, respectively. The structure of **P4-NEM** is characterized by the series of b3–b6, b8, b9, b11, and b12 fragment ions, and multiple internal fragment ions (e.g., $EIQLu_1$, u_1HNLG) (Figure 14). The latter demonstrate that the homocysteine residue (labeled "u_1" in the sequence) is derivatized with NEM. The y1–y3 fragment ions allow the identification of the C-terminal lysine (labeled "u_2" in the sequence) as the second residue derivatized with NEM. Noteworthy, the conversion of Met[8] into homocysteine was observed along with the formation of **P2**. In contrast, when PTH(1-34) was oxidized under conditions where **P2** was not observed, no transformation of Met[8] into homocysteine was observed either. Those results point to a common intermediate in the formation of the hydrolysis product **P2** and the homocysteine-containing product **P4**. However, when PTH-(1-34) was oxidized in the presence of MeOH (1 M) or in the absence of H_2O_2, only the formation of **P2** but not that of **P4** was detected.

4. DISCUSSION

To predict oxidation and stability problems for protein pharmaceuticals, more detailed mechanistic studies are necessary, which characterize and quantify oxidation products for specific oxidation pathways as a function of peptide and protein sequence and conformational properties. Such mechanistic studies are here presented for the Fenton

oxidation of parathyroid hormone (1-34), PTH(1-34), a suitable model protein, which contains a number of oxidizable amino acids such as His, Met, Trp, and Tyr. [25] For our experiments, the individual components of the Fenton reaction, $[Fe^{II}(EDTA)]^{2-}$(EDTA = ethylenediaminetetraacetate), H_2O_2, and PTH(1-34) were prepared under Ar to maintain a set of defined and reproducible reaction conditions. Subsequently, these components were combined either under Ar or air to assess the influence of O_2 on the oxidation yields. These conditions are different to those of Ji et al.,[25] who prepared PTH(1-34), $FeCl_2$ and H_2O_2 without EDTA under air. The latter conditions do not allow for an appropriate characterization of the involvement of molecular oxygen in the oxidation mechanisms of PTH(1-34). Thus, comparative studies under Ar and air are mandatory. Under Ar, the presence of EDTA allows to start the reaction with a defined complex of Fe^{II}, that is, $[Fe^{II}(EDTA)]^{2-}$, while in the absence of EDTA various complexes of Fe^{II} may be present at the start of the reaction, potentially involving the buffer and multiple binding sites of PTH(1-34). An additional problem with Ji's preparation is, that in oxygen-containing solution Fe^{II} will convert rapidly into Fe^{III}, so that the actual concentration of Fe^{II} at the time point of H_2O_2 addition to the solution may be negligible. Instead, in our experiments we prepared $[Fe^{II}(EDTA)]^{2-}$ under Ar, prior to the addition of $[Fe^{II}(EDTA)]^{2-}$ into a solution containing either O_2 or O_2 and H_2O_2 to start the reaction.

For mechanistic purposes, in this study, either selected components of our Fenton system were omitted (controls) or oxygen was admitted to the reaction mixture after the addition of $[Fe^{II}(EDTA)]^{2-}$ to PTH(1-34) under Ar. These experimental variations led to the characterization of a complex oxidation mechanism, where the reaction of $[Fe^{II}(EDTA)]^{2-}$/H_2O_2 with PTH(1-34) leads to the oxidation of predominantly His and Met, but the exposure of PTH(1-34) to $[Fe^{II}(EDTA)]^{2-}$ and O_2 (in the absence of H_2O_2) resulted in the specific hydrolysis of the peptide bond between Met-8 and His-9. This hydrolysis reaction is prevented in a PTH(1-34) mutant, in which Met[8] is replaced by Ala[8], referred to as PTH(1-34)Met[8]Ala, and by replacement of EDTA with diethylenetriaminepentaacetate (DTPA). In contrast, the replacement of EDTA by DTPA had no significant effect on the oxidation yields from Met and His, in accordance with the fact that H_2O_2 reacts with both $[Fe^{II}(EDTA)]^{2-}$ and $[Fe^{II}(DTPA)]^{3-}$, albeit the rate constant for reaction with $[Fe^{II}(EDTA)]^{2-}$ (reaction 1) is an order of magnitude higher compared to that with $[Fe^{II}(DTPA)]^{3-}$.[18,26] An important difference between the two chelators EDTA and DTPA is the availability of eight metal-binding coordination sites in DTPA compared with six coordination sites in EDTA. The crystal structure of $[Fe^{II}(EDTA)]^{2-}$ demonstrates that the central Fe^{II} ion is complexed by seven ligands, six EDTA-derived ligands, and one water molecule,[27] which would explain the high reactivity with H_2O_2. In contrast, DTPA binds to iron through a heptavalent complex[28] that saturates all potentially valencies in $[Fe^{II}(DTPA)]^{3-}$. Hence, the reaction of H_2O_2 with $[Fe^{II}(DTPA)]^{3-}$ would require the dissociation of one of the coordinating ligands, rationalizing the faster reaction of H_2O_2 with $[Fe^{II}(EDTA)]^{2-}$ compared to $[Fe^{III}(EDTA)]^{3-}$. Here the heptacoordination by DTPA compared to hexacoordination by EDTA is likely also the reason for the higher stability constants of the DTPA vs EDTA complexes, where the individual stability constants $\log(K_{ML})$ are given in parentheses: Fe^{II}-EDTA (14.33), Fe^{III}-EDTA (25.1), Fe^{II}-DTPA (16.50), Fe^{III}-DTPA (28.6).[29,30]

The Fenton reaction between Fe^{II} and H_2O_2 involves various intermediates, where H_2O_2 first adds to Fe^{II}, prior to the formation of Fe^{III} and a free hydroxyl radical (reactions 1–4, representatively shown for $[Fe^{II}(EDTA)]^{2-}$).[18,31–33] $[Fe^{II}(EDTA)]^{2-}$ is extremely oxygen-sensitive.[28] In the presence of O_2, $[Fe^{II}(EDTA)O_2]^{2-}$ can be converted through an acid-catalyzed electron-transfer process in $[Fe^{III}(EDTA)]^{-}$ and $HO_2^{\bullet}(\rightleftarrows H^+ + O_2^{\bullet-})$. Here, acidic conditions lead to the protonation of EDTA in $[Fe^{II}(EDTA)(H_2O)]^{2-}$ (reaction 5) resulting into a change of the geometry of the complex. The new complex, $[Fe^{II}(EDTAH)(H_2O)]^{-}$, is

a pentagonalbipyramidal species that can bind more rapidly to O_2 than the nonprotonated and deprotonated monocapped trigonalprismatic species.[34,35]

$$\left[Fe^{II}(EDTA)\right]^{2-} + H_2O_2 \rightarrow \left[Fe^{II}(EDTA)(H_2O_2)\right]^{2-} \quad (1)$$

$$\left[Fe^{II}(EDTA)(H_2O_2)\right]^{2-} \rightarrow \left[Fe^{IV}(EDTA)(HO)\right]^{-} + HO^{-} \quad (2)$$

$$\left[Fe^{II}(EDTA)(O_2)\right]^{-} + H_2O \rightarrow \left[Fe^{IV}(EDTA)(HO)\right]^{-} + HO_2 \quad (3)$$

$$\left[Fe^{II}(EDTA)(HO_2)\right]^{2-} + H_2O \rightarrow \left[Fe^{III}(EDTA)(HO)\right]^{-} + HO^{-} + HO^{\bullet} \quad (4)$$

$$\left[Fe^{II}(EDTA)(H_2O)\right]^{2-} + H^{+} \rightarrow \left[Fe^{II}(EDTAH)(H_2O)\right]^{-} \quad (5)$$

$$\left[Fe^{II}(EDTAH)(H_2O)\right]^{-} + O_2 \rightarrow \left[Fe^{II}(EDTAH)(O_2)\right]^{-} + H_2O \quad (6)$$

The Fe^{II}-EDTA intermediates presented in reactions 1–6, as well as the hydroxyl radical, and $[Fe^{III}(EDTA)(OH)]^{-}$ will react with amino acids of PTH(1-34) to different extents, depending on the nature of the intermediates. In addition, a possible association of PTH(1-34) with the initial $[Fe^{II}(EDTA)]^{2-}$ complex or some of the intermediates, for example, $[Fe^{II}(EDTAH)O_2]^{-}$, must be considered, potentially localizing the reactive intermediates to specific sites of PTH(1-34). Such association can be through coordination of the metal to an appropriate amino acid side chain (e.g., of His). In addition, the electrostatic interaction of EDTA with His has been documented by ^1H NMR studies, for example, for bovine pancreatic ribonuclease,[36] suggesting that overall negatively charged complexes of Fe^{II} and Fe^{III} with EDTA and DTPA may show similar interactions with other proteins.

PTH(1-34) was easily modified under air in the presence of $[Fe^{II}/EDTA]^{2-}$. These conditions resulted in a hydrolytic cleavage between Met[8] and His[9], which depended on the presence of Fe^{II} and O_2. Importantly, the presence of H_2O_2 increased the yield of oxidation of Met[8] into MetSO but lowered the hydrolysis of the peptide bond between Met[8] and His[9]. In addition, the presence of exogenous Met during the oxidation of PTH(1-34) or the mutation of Met[8] to Ala[8] prevented the hydrolytic reaction. In addition to these observations, the oxidation of Met[8] into MetSO prevented the hydrolytic reaction. These observations suggest that an unmodified sulfur in Met[8] is required to initiate the formation of an intermediate, which can lead to the hydrolysis of the peptide bond Met[8]–His[9]. This intermediate is most likely an oxidized sulfur, such as the sulfide radical cation **C2** displayed in Scheme 1. The formation of such an oxidized intermediate is consistent with the protective role of exogenous Met (competing for the oxidizing species) and also the formation of product **P4** (see Scheme 2). We observed that Met[18], Trp[23], and His[32] were hardly oxidized under our experimental conditions. Besides, no hydrolytic cleavage around the residues Met[18] and His[32] was observed. Such observations indicate that the proximity (in space and in the sequence) of the residues Met and His promotes the hydrolysis of the peptide bond that links these two residues.

In the following, we will rationalize our experimental results to explain how molecular oxygen, Fe^{II}, Met[8] and His[9] can interact to drive the cleavage of the peptide bond between Met[8] and His[9]. Our hypothesis is that the hydrolytic reaction can occur in a complex involving PTH(1-34) (likely through His[9]) and a peroxo-iron species. The involvement of His coordination in the formation of **P2** is suggested by the observed pH-dependency, where no formation of **P2** was observed at pH 4.5, that is, when the His residue was protonated. A preliminary discussion about the possible nature of the peroxo-iron complex is, therefore, mandatory to explain the mechanism leading to the specific hydrolysis of the peptide bond between Met[8] and His[9].

The Primary Oxidizing Species

Experiments under Ar—The precursors leading to the oxidizing species are presented in reactions 1–6, where the addition of H_2O_2 to $[Fe^{II}/EDTA]^{2-}$ (reaction 1, $k_1 = 7–17.5 \times 10^3$ M^{-1} s^{-1}),[26] is followed by the elimination of a molecule of HO^- or H_2O (reactions 2 and 3).[18,31–33] Any of these iron-oxo complexes generated through reactions 2 and 6 are able to react through either electron transfer or hydrogen-atom abstraction with substrates, here PTH(1-34).[18,33,37,38]

Experiments under Air—The presence of O_2 can change the nature of the intermediates leading to the primary oxidizing species. The oxidation of aqueous Fe^{II}, Fe^{II}_{aq}, can be written as an O_2^- and HO^--dependent reaction (reaction 7) with an oxidation rate described by eq E1 in the pH range 4–8 (in bicarbonate solutions).[39]

$$Fe^{II}_{aq} + O_2 + 2HO^- + H_2O \rightarrow Fe(OH)_3 + HO_2^{\bullet} \quad (7)$$

$$\frac{-d\left[Fe^{II}\right]}{dt} = k_5 \left[Fe^{II}\right] P_{O_2} \left[HO^-\right]^2 \quad (E1)$$

If the oxidation of Fe^{II}_{aq} is only described by reaction 7 (and eq E1), the primary oxidizing species is $HO_2^{\bullet}/O_2^{\bullet-}$, or the dismutation product, H_2O_2 (reaction 8).

$$2O_2^{\bullet-} + 2H^+ \rightarrow H_2O_2 + O_2 \quad (8)$$

However, reaction 7 has to be re-evaluated when ferrous iron is chelated. Indeed, the reaction order on Fe^{II}_{aq} may vary from first to second order. This reaction order dependency can be related to the pH and concentration of the Fe^{II} chelate. In the presence of chelators such as EDTA, DTPA, and nitrilotriacetate (NTA) there is general agreement that above pH 6 the reaction with O_2 is pH-independent.[40–43] Zang and van Eldik have determined a kinetic order of 1 and 1–2 with regard to O_2 and Fe^{II}, respectively[40] under the following conditions: (i) 25 μM < $[Fe^{II}]$ < 20 mM, (ii) 50 μM < [EDTA] < 20 mM, (iii) 125 μM < $[O_2]$ < 1.25 mM, (iv) 2 < pH < 7. The increase of the order of reaction in ferrous chelate with increasing concentrations of ferrous chelate is explained by reactions 9–13 (where L represents a chelator).[40] A short discussion about the order of the reaction on ferrous iron and oxygen is warranted if we want to evaluate the degree of oxidation of iron in the $[Fe^{II}(EDTA)]^{2-}/O_2$ complex under our experimental conditions.

$$Fe^{II}L^{n-} + O_2 \rightleftarrows Fe^{II}O_2L^{n-} \quad (9)$$

$$Fe^{II}O_2L^{n-} \rightarrow Fe^{III}L^{n-} + O_2^{\bullet -} \quad (10)$$

$$Fe^{II}O_2L^{n-} + Fe^{II}L^{n-} + 2H^+ \rightarrow 2Fe^{III}L^{n-} + H_2O_2 \quad (11)$$

$$Fe^{II}L^{n-} + O_2^- + 2H^+ \rightarrow Fe^{III}L^{n-} + H_2O_2 \quad (12)$$

$$2Fe^{II}L^{n-} + H_2O_2 + 2H^+ \rightarrow 2Fe^{III}L^{n-} + 2H_2O \quad (13)$$

At the lowest concentration of ferrous chelate (≤100 μM), reaction 8 is likely to be rate-controlling, while reaction 11 is negligible. An increase of the concentration of ferrous chelate should promote reaction 11 such that, at some point, it will compete against reaction 10, resulting in a change of the order of the reaction from one to two.

Thus, the rate constant for the oxidation of $[Fe^{II}(EDTA)]^{2-}$ by O_2 can be estimated to be either between 20 and 300 M^{-1} s^{-1} at pH 6 in the presence of excess oxygen (with a first-order reaction on $[Fe^{II}(EDTA)]^{2-}$)[34,44] or between 6.5 and 18 × 10^3 M^{-2} s^{-1} for a pH range 5–7.5 in the presence of an excess of $[Fe^{II}(EDTA)]^{2-}$ (with the reaction being second order with regard to $[Fe^{II}(EDTA)]^{2-}$).[40,45]

Importantly, under our conditions of oxidation of PTH(1-34), with $[Fe^{II}(EDTA)]^{2-}$ = 100 μM, the major oxidizing species is likely a peroxo-iron complex, as referred to in equilibrium 14, and illustrated in Scheme 1.

Hydrolysis of the Peptide Bond between Met[8] and His[9]

The hydrolysis of the peptide bond between Met[8] and His[9] requires Fe^{II}, O_2, and a pH at which the imidizole nitrogen is deprotonated (**P2** was not formed at pH 4.5 in Exp 5), consistent with the necessity of the imidazole side chain for coordination of Fe^{II}. The hydrolysis proceeds in the presence of EDTA but not DTPA and proceeds in the presence of acetate but not phosphate. Our results show that the formation of **P2** is inhibited through the oxidation of Met[8] and that H_2O_2 is not required for hydrolysis (Figures 6B vs D and 8). The replacement of Met[8] by Ala[8] in the PTH(1-34)Met[8]Ala mutant as well as the preoxidation of Met[8] into MetSO prevent the hydrolysis of the peptide bond between Met[8] (or Ala[8]) and His[9] in PTH(1-34) (and the PTH(1-34) Met[8]/Ala mutant). These results suggest that the hydrolysis between Met[8] and His[9] requires an unmodified Met sulfur. We believe that the role of this intact sulfur is not coordination of Fe^{II} but the formation of sulfide radical cations as precursors for hydrolysis.

The formation of **P2** is also prevented by (i) chelation of Fe^{II} with DTPA (instead of EDTA) (Exp. 2, Figures 3 and 6C), (ii) replacing $[Fe^{II}/EDTA]^{2-}$ by $[Fe^{III}/EDTA]^-$ (data not shown), (iii) performing the reaction under Ar and chelation of Fe^{II} with DTPA prior to exposure of the solution to air (Exp. 6, Figure 8A), and (iv) the addition of exogenous Met to the solution. While **P2** is not formed in the presence of $[Fe^{II}/EDTA]^{2-}$ under Ar (Figure 7B), **P2** is formed when PTH(1-34) is exposed to air prior to the addition of DTPA (Figure 7A).

Based on all the experimental observations, we propose the mechanism detailed in Scheme 1. Complexation of $[Fe^{II}(EDTA)]^{2-}$ to His[9], followed by oxygen addition to Fe^{II}, leads to a metal-bound peroxyl radical, **C1**. This peroxyl radical oxidizes the Met[8] sulfur via one-electron transfer to yield **C2** and a ferrous superoxo complex (reaction 14). While the

possibility for back electron transfer exists, the intermediary sulfide radical cation will complex with the peptide bond carbonyl function to form a cyclic, three-electron-bonded intermediate **C3** (equilibrium 15). Evidence for such cyclic sulfur–oxygen bonded intermediates has been documented for various peptides by time-resolved spectroscopic analysis during pulse radiolysis experiments.[46,47] In intermediate **C3**, the complexation of the carbonyl function by the positively charged sulfide radical cation can be compared to the complexation of the peptide bond by other Lewis acids such as H^+ or transition metals, which leads to hydrolysis of the peptide bond.[48–51] In fact, kinetic analysis of the stability of sulfur–oxygen three-electron bonded intermediates in peptides have strongly suggested a hydrolysis reaction[52] analogous to that depicted in reaction 16. Subsequently, the remaining sulfur radical cation $\mathbf{I}_1$ can be reduced back by the ferrous superoxo complex (reaction 17), regenerating the initial $Fe^{II}(Ln)OO^{\bullet}$ species.

The hydrolysis process in Scheme 1 is consistent with our experimental observation of O^{18} incorporation into product **P2** (which results in the shift of its *m/z* 906.4–908.4, Figure 12) when the oxidation reaction is performed in H_2O^{18}. Importantly, the hydrolysis cannot be inhibited by the addition of CH_3OH at sufficient concentrations to scavenge hydroxyl radicals. This result is consistent with the mechanism in Scheme 1, which does not involve hydroxyl radicals, and with the fact that O_2, but not H_2O_2 (the precursor for hydroxyl radicals) is required for the hydrolysis reaction. The necessity for an unoxidized Met residue for hydrolysis is further indicated by our observation that (i) the replacement of Met[8] by Ala[8], (ii) the oxidation of Met[8] to MetSO, and (iii) the addition of exogenous Met prevented the hydrolysis reaction.

The hydrolysis mechanism observed under our experimental conditions is different from those reported by Rana and Meares,[53] where reaction between $[Fe^{III}(EDTA)]^-$ and H_2O_2 led to a nucleophile which attacked the peptide bond. Our mechanism clearly requires Met oxidation and is directed via complexation of Fe^{II} to His[9] or Met[8]. From a pharmaceutical viewpoint, the fact that the addition of EDTA cannot prevent the hydrolysis is important, as EDTA is frequently used as a chelator to prevent metal-catalyzed reactions in formulations.[54] We did not observe the hydrolysis of the peptide bond between Met[8] and His[9] in the presence of phosphate buffer. We did not investigate in detail the reason why the hydrolysis did not occur in the presence of phosphate. Mechanistic evidence suggests a complex formation between phosphate and sulfide radical cations, which may interfere with equilibrium 15 and, consequently, with the hydrolysis reaction.[55] We know that phosphate can have a significant influence on the chemistry of sulfide radical cations.[55] We tentatively rationalize the inhibition of hydrolysis by phosphate with the complexation of the sulfide radical cation by phosphate.

Formation of Homocysteine

The formation of homocysteine proceeds under experimental conditions, which also promote the hydrolysis between Met[8] and His[9], consistent with our hypothesis of a common intermediate. In fact, the deprotonation of methionine radical cation C2 generates two types of carbon-centered radicals, of which C5 represents a precursor for homocysteine (reaction 18, Scheme 2).[56] In the presence of air, C5 can react with O_2 to form a peroxyl radical, which ultimately leads to the formation of homocysteine (reactions 19–22, Scheme 2).

Oxidation of Met[8] and His[9]

After oxidation of PTH(1-34) in Ar at pH 6.9 and 7.8, and in accordance with the experimental protocol Exp.5, we observed the oxidation of Met[8] and His[9] into MetSO and 2-oxo-histidine, respectively. Changing the pH to pH 4.5 under otherwise similar

conditions, led to complete conversion of Met[8] into MetSO (monitored through the ratio **P1/F5** = 100%). This result indicates that complexation of Fe^{II} by His is not necessary for the oxidation of Met into MetSO by $[Fe^{II}(EDTA)]^{2-}/H_2O_2$, consistent with earlier studies on oxidation of Met-containing peptides, which did not contain His.[16,31] The quantitation of the oxidation yield of His[9] in wild type PTH was not possible since its oxidation was accompanied by the oxidation of Met[8]. However, in the PTH mutant, the absence of Met[8] allows for the quantitation of oxidation of His[9]. The conversion of His[9] into 2-oxo-histidine in PTH-Met[8]/Ala[8] amounts to ca. 2%.

Oxidation of Met[18], W[23], and His[32]

Our results show that Met[18], W[23], and His[32] are not prone to significant oxidation under our experimental conditions. While traces of their oxidation products are observed, their yields are negligible in comparison to the yields of **P1** and **P2**. In contrast, Ji et al.[25] reported significant oxidation on Met[18] and W[23] during metal-catalyzed oxidation of PTH for 24 h (at 40 °C) in air-saturated solutions containing $FeCl_2$ and H_2O_2. We believe that the differential sensitivity of Met[8] and Met[18] toward oxidation may be, in part, caused by secondary structure. The NMR structures[57] of PTH(1-34) show that Met[8] is located in an α helix whereas Met[18] is not. Our theoretical and experimental studies[58,59] have shown that a Met residue located within an α-helix can be more sensitive toward oxidation as compared to a Met residue located outside an α-helix. This is due to the facile complex formation between a sulfide radical cation and the peptide bond of the amino acid residue in position i-4.

Significance

Frequently, EDTA is added to pharmaceutical formulations in an attempt to prevent peptide and protein oxidation. The current results demonstrate that Fe^{II}/H_2O_2, $[Fe^{II}(EDTA)]^{2-}/H_2O_2$, Fe^{II}/O_2, and $[Fe^{II}(EDTA)]^{2-}/O_2$ have the potential to oxidize Met and/or His in PTH(1-34). Hence, these data provide evidence that the addition of EDTA may not always protect a peptide or protein from oxidation. Importantly, Met sulfoxide is not the only oxidation product of Met[8], which also converts to homocysteine. Moreover, both in the absence and presence of EDTA, Fe^{II} catalyzes the site-specific cleavage of the peptide bond between Met[8] and His[9], a mechanism likely depending on the intermediary formation of a one-electron oxidized Met residue. We note that the Fe^{II}/Fe^{III} concentrations used in our experiments are significantly higher than those one would expect in pharmaceutical formulations. Hence, the yield of hydrolysis/oxidation products under formulation conditions can be expected to be lower. Our results further substantiate that Fe^{III}, the iron species pharmaceutical preparation most frequently encountered, will generate predominantly methionine sulfoxide, not hydrolysis. However, Fe^{II} may be generated through the reaction of Fe^{III} with contaminating peroxides, providing a potential route to hydrolysis. The question is whether the addition of EDTA can actually promote such hydrolytic processes in larger proteins such as antibodies, for example through keeping Fe^{II} (or Fe^{III}) in solution.

5. CONCLUSION

Under relatively mild metal-catalyzed oxidation conditions, the oxidation of PTH(1-34) is site-specific. Only Met[8] and His[9] are readily oxidized under conditions where all six amino acid residues, Met[8], His[9], Met[18], Trp[23], His[32], and Phe[34] could have been oxidized. A one-electron oxidized intermediate, a radical cation of Met[8] leads to a selective hydrolytic cleavage between Met[8] and His[9]. We hypothesize that the particular spatial conformation of Met[8] and His[9] renders this region sensitive to metal-catalyzed oxidation and hydrolysis. The radical cation of Met[8] is likely at the origin of the

transformation of Met[8] into homocysteine. However, the conversion of Met[8] into homocysteine can be prevented by the addition of MeOH, without interfering with the hydrolytic cleavage between Met[8] and His[9]. This result would suggest that HO• radicals are involved in the transformation of Met[8] into homocysteine.

Supplementary Material

Refer to Web version on PubMed Central for supplementary material.

Acknowledgments

We gratefully acknowledge Mary Cromwell's support of this project and financial support from Genentech, the NIH (P01AG12993), and NSF (CHE-0956581).

REFERENCES

1. Cederbaum S, Vilain E. Defects in energy metabolism: coming of age, slowly. J. Pediatr. 2000; 136(2):147–8. [PubMed: 10657817]
2. Stadtman ER. Protein modification in aging. J. Gerontol. 1988; 43(5):B112–20. [PubMed: 3047204]
3. Ozben, T.; Chevion, M. Frontiers in Neurodegenerative Disorders and Aging: Fundamental Aspects, Clinical Perspectives and New Insights. NATO Science Series ed.. IOS Press; Amsterdam: 2004.
4. Manning MC, Chou DK, Murphy BM, Payne RW, Katayama DS. Stability of protein pharmaceuticals: an update. Pharm. Res. 2010; 27(4):544–575. [PubMed: 20143256]
5. Toennies G, Callan TP. Methionine studies: III. A comparison of oxidative reactions of methionine, cysteine, and cystine. Determination of methionine by hydrogen peroxide oxidation. J. Biol. Chem. 1939; 129(2):481–490.
6. Cuq JL, Besancon P, Chartier L, Cheftel C. Oxidation of Methionine Residues of Food Proteins and Nutritional Availability of Protein-Bound Methionine Sulfoxide. Food Chem. 1978; 3(2):85–102.
7. Cuq JL, Provansa M, Guilleux F, Cheftel C. Oxidation of Methionine Residues of Casein by Hydrogen-Peroxide–Effects on in-Vitro Digestibility. J. Food Sci. 1973; 38(1):11–13.
8. Ellinger GM. Chemical Approach to Nutritional Availability of Methionine in Food Proteins. Ann. Nutr. Aliment. 1978; 32(2−3):281–289. [PubMed: 707916]
9. Goldstein S, Meyerstein D, Czapski G. The Fenton reagents. Free Radical Biol. Med. 1993; 15(4): 435–445. [PubMed: 8225025]
10. Davies MJ. The oxidative environment and protein damage. Biochim. Biophys. Acta. 2005; 1703(2):93–109. [PubMed: 15680218]
11. Levine RL, Mosoni L, Berlett BS, Stadtman ER. Methionine residues as endogenous antioxidants in proteins. Proc. Natl. Acad. Sci. U.S.A. 1996; 93(26):15036–15040. [PubMed: 8986759]
12. Zhao F, Ghezzo-Schöneich E, Aced GI, Hong JY, Milby T, Schöneich C. Metal-catalyzed oxidation of histidine in human growth hormone - Mechanism, isotope effects, and inhibition by a mild denaturing alcohol. J. Biol. Chem. 1997; 272(14):9019–9029. [PubMed: 9083026]
13. Levine RL. Oxidative Modification of Glutamine-Synthetase. 1. Inactivation Is Due to Loss of One Histidine Residue. J. Biol. Chem. 1983; 258(19):1823–1827.
14. Li S, Nguyen TH, Schöneich C, Borchardt RT. Aggregation and precipitation of human relaxin induced by metal-catalyzed oxidation. Biochemistry. 1995; 34(17):5762–5772. [PubMed: 7727437]
15. Lam XM, Lai WG, Chan EK, Ling V, Hsu CC. Site-Specific Tryptophan Oxidation Induced by Autocatalytic Reaction of Polysorbate 20 in Protein Formulation. Pharm. Res. 2011; 28(10):2543–2555. [PubMed: 21656082]
16. Hong J, Schöneich C. The metal-catalyzed oxidation of methionine in peptides by Fenton systems involves two consecutive one-electron oxidation processes. Free Radical Biol. Med. 2001; 31(11): 1432–41. [PubMed: 11728815]
17. Torosantucci R, Mozziconacci O, Sharov V, Schöneich C, Jiskoot W. Chemical Modifications in Aggregates of Recombinant Human Insulin Induced by Metal-Catalyzed Oxidation: Covalent

Cross-Linking via Michael Addition to Tyrosine Oxidation Products. Pharm. Res. 2012; 29(8): 2276–2293. [PubMed: 22572797]

18. Rush JD, Koppenol WH. The reaction between ferrous polyaminocarboxylate complexes and hydrogen peroxide: an investigation of the reaction intermediates by stopped flow spectrophotometry. J. Inorg. Biochem. 1987; 29(3):199–215. [PubMed: 3106570]
19. Ikehata K, Duzhak TG, Galeva NA, Ji T, Koen YM, Hanzlik RP. Protein targets of reactive metabolites of thiobenzamide in rat liver in vivo. Chem. Res. Toxicol. 2008; 21(7):1432–42. [PubMed: 18547066]
20. Xu H, Freitas MA. MassMatrix: a database search program for rapid characterization of proteins and peptides from tandem mass spectrometry data. Proteomics. 2009; 9(6):1548–55. [PubMed: 19235167]
21. Xu H, Freitas MA. A mass accuracy sensitive probability based scoring algorithm for database searching of tandem mass spectrometry data. BMC Bioinform. 2007; 8:133.
22. Xu H, Yang L, Freitas MA. A robust linear regression based algorithm for automated evaluation of peptide identifications from shotgun proteomics by use of reversed-phase liquid chromatography retention time. BMC Bioinform. 2008; 9:347.
23. Xu H, Zhang L, Freitas MA. Identification and characterization of disulfide bonds in proteins and peptides from tandem MS data by use of the MassMatrix MS/MS search engine. J. Proteome Res. 2008; 7(1):138–44. [PubMed: 18072732]
24. Khossravi M, Borchardt RT. Chemical pathways of peptide degradation: IX. Metal-catalyzed oxidation of histidine in model peptides. Pharm. Res. 1998; 15(7):1096–1102. [PubMed: 9688066]
25. Ji JA, Zhang BY, Cheng W, Wang YJ. Methionine, Tryptophan, and Histidine Oxidation in a Model Protein, PTH: Mechanisms and Stabilization. J. Pharm. Sci. 2009; 98(12):4485–4500. [PubMed: 19455640]
26. Rush JD, Maskos Z, Koppenol WH. Distinction between hydroxyl radical and ferryl species. Methods Enzymol. 1990; 186:148–156. [PubMed: 2172702]
27. Mizuta T, Wang J, Miyoshi K. A Seven-Coordinate Structure of Iron(II)−Ethylenediamine-N,N,N′,N′-tetraacetato Complex as Determined by X-Ray Crystal Analysis. Bull. Chem. Soc. Jpn. 1993; 66(9):2547–2551.
28. Finnen DC, Pinkerton AA, Dunham WR, Sands RH, Funk MO. Structures and Spectroscopic Characteristics of Iron(III) Diethylenetriaminepentaacetic Acid Complexes - a Nonheme Iron(III) Complex with Relevance to the Iron Environment in Lipoxygenases. Inorg. Chem. 1991; 30(20): 3960–3964.
29. Ureno, K.; Imamura, T.; Chang, KL. CRC Handbook of Organic Analytical Reagents. CRC Press; Boca Raton, FL: 1992.
30. Inczédy, J. Analytical Applications of Complex Equilibria. E. Horwood; Chichester, England: 1976.
31. Schöneich C, Yang J. Oxidation of methionine peptides by Fenton systems: the importance of peptide sequence, neighboring groups and EDTA. J. Chem. Soc., Perkin Trans. 2. No. 1996; 5:915–924.
32. Rush JD, Koppenol WH. Oxidizing intermediates in the reaction of ferrous EDTA with hydrogen peroxide. Reactions with organic molecules and ferrocytochrome c. J. Biol. Chem. 1986; 261(15): 6730–6733. [PubMed: 3009473]
33. Rahhal S, Richter HW. Reduction of hydrogen peroxide by the ferrous iron chelate of diethylenetriamine-N,N,N′,N″,N″-pentaacetate. J. Am. Chem. Soc. 1988; 110(10):3126–3133.
34. Seibig S, van Eldik R. Kinetics of [FeII(edta)] Oxidation by Molecular Oxygen Revisited. New Evidence for a Multistep Mechanism. Inorg. Chem. 1997; 36(18):4115–4120.
35. Meier R, Heinemann FW. Structures of the spontaneously resolved six-coordinate potassium chloro-(ethylenediaminetriacetato acetic acid) iron(III) monohydrate and the seven-coordinate potassium (ethylenediaminetetracetato) iron(III) sesquihydrate. Inorg. Chem. Acta. 2002; 337:317–327.
36. Brauer M, Benz FW. ^{1}H NMR studies of the binding of EDTA to bovine pancreatic ribonuclease. Biochim. Biophys. Acta. 1978; 533(1):186–94. [PubMed: 416852]

37. Rush JD, Koppenol WH. Reactions of iron(II) nitrilotriacetate and iron(II) ethylenediamine-N,N′-diacetate complexes with hydrogen peroxide. J. Am. Chem. Soc. 1988; 110(15):4957–4963.
38. Yamazaki I, Piette LH. EPR spin-trapping study on the oxidizing species formed in the reaction of the ferrous ion with hydrogen peroxide. J. Am. Chem. Soc. 1991; 113(20):7588–7593.
39. Stumm W, Lee GF. Oxygenation of Ferrous Iron. Ind. Eng. Chem. 1961; 53(2):143–146.
40. Zang V, Vaneldik R. Kinetics and Mechanism of the Autoxidation of Iron(II) Induced through Chelation by Ethylenediaminetetraacetate and Related Ligands. Inorg. Chem. 1990; 29(9):1705–1711.
41. Sada E, Kumazawa H, Machida H. Oxidation-Kinetics of Fe-II-Edta and Fe-II-Nta Chelates by Dissolved-Oxygen. Ind. Eng. Chem. Res. 1987; 26(7):1468–1472.
42. Bull C, Mcclune GJ, Fee JA. The Mechanism of Fe-Edta Catalyzed Superoxide Dismutation. J. Am. Chem. Soc. 1983; 105(16):5290–5300.
43. Kurimura Y, Ochiai R, Matsuura N. Oxygen Oxidation of Ferrous Ions Induced by Chelation. Bull. Chem. Soc. Jpn. 1968; 41(10):2234–2239.
44. Brown ER, Mazzarella JD. Mechanism of Oxidation of Ferrous Polydentate Complexes by Dioxygen. J. Electroanal. Chem. 1987; 222(1−2):173–192.
45. Wubs HJ, Beenackers AACM. Kinetics of the oxidation of ferrous chelates of EDTA and HEDTA in aqueous solution. Ind. Eng. Chem. Res. 1993; 32(11):2580–2594.
46. Schöneich C, Pogocki D, Hug G, Bobrowski K. Free radical reactions of methionine in peptides: mechanisms relevant to beta-amyloid oxidation and Alzheimer's disease. J. Am. Chem. Soc. 2003; 125(45):13700–13. [PubMed: 14599209]
47. Schöneich C, Pogocki D, Wisniowski P, Hug GL, Bobrowski K. Intramolecular Sulfur−Oxygen Bond Formation in Radical Cations of N-Acetylmethionine Amide. J. Am .Chem. Soc. 2000; 122(41):10224–10225.
48. Chin J. Developing artificial hydrolytic metalloenzymes by a unified mechanistic approach. Acc. Chem. Res. 1991; 24(5):145–152.
49. Milović NM, Dutcă L-M, Kostić NM. Transition-Metal Complexes as Enzyme-Like Reagents for Protein Cleavage: Complex cis-$[Pt(en)(H_2O)_2]^{2+}$ as a New Methionine-Specific Protease. Chem.–Eur. J. 2003; 9(20):5097–5106. [PubMed: 14562327]
50. Milovic NM, Kostic NM. Interplay of terminal amino group and coordinating side chains in directing regioselective cleavage of natural peptides and proteins with palladium(II) complexes. Inorg. Chem. 2002; 41(26):7053–63. [PubMed: 12495344]
51. Milović NM, Kostić NM. Palladium(II) complexes, as synthetic peptidases, regioselectively cleave the second peptide bond “upstream” from methionine and histidine side chains. J. Am. Chem. Soc. 2002; 124(17):4759–69. [PubMed: 11971725]
52. Bobrowski K, Hug GL, Pogocki D, Marciniak B, Schöneich C. Stabilization of Sulfide Radical Cations through Complexation with the Peptide Bond: Mechanisms Relevant to Oxidation of Proteins Containing Multiple Methionine Residues. J. Phys. Chem. B. 2007; 111(32):9608–9620. [PubMed: 17658786]
53. Rana TM, Meares CF. Transfer of oxygen from an artificial protease to peptide carbon during proteolysis. Proc. Natl. Acad. Sci. U.S.A. 1991; 88(23):10578–82. [PubMed: 1961724]
54. Zhou S, Zhang B, Sturm E, Teagarden DL, Schöneich C, Kolhe P, Lewis LM, Muralidhara BK, Singh SK. Comparative Evaluation of Disodium Edetate and Diethylenetriaminepentaacetic Acid as Iron Chelators to Prevent Metal-Catalyzed Destabilization of a Therapeutic Monoclonal Antibody. J. Pharm. Sci. 2010; 99(10):4239–50. [PubMed: 20737631]
55. Schöneich C, Miller BL, Hug GL, Bobrowski K, Marciniak B. Intermolecular Complexes Between Sulfide Radical Cations from β-Hydroxy Sulfides and Phosphate. Res. Chem. Intermed. 2001; 27(1,2):165–175.
56. Hiller KO, Masloch B, Göbl M, Asmus KD. Mechanism of the OH• Radical Induced Oxidation of Methionine in Aqueous Solution. J. Am. Chem. Soc. 1981; 103(10):2734–2743.
57. Marx UC, Adermann K, Bayer P, Forssmann W-G, Rösch P. Solution Structures of Human Parathyroid Hormone Fragments hPTH(1-34) and hPTH(1-39) and Bovine Parathyroid Hormone Fragment bPTH(1-37). Biochem. Biophys. Res. Commun. 2000; 267(1):213–220. [PubMed: 10623601]

58. Pogocki D, Schöneich C. Redox Properties of Met(35) in Neurotoxic Beta-Amyloid Peptide. A Molecular Modeling Study. Chem. Res. Toxicol. 2002; 15(3):408–18. [PubMed: 11896689]

59. Kanski J, Aksenova M, Schoneich C, Butterfield DA. Substitution of Isoleucine-31 by Helical-Breaking Proline Abolishes Oxidative Stress and Neurotoxic Properties of Alzheimer's Amyloid Beta-Peptide. Free Radical Biol. Med. 2002; 32(11):1205–1211. [PubMed: 12031904]

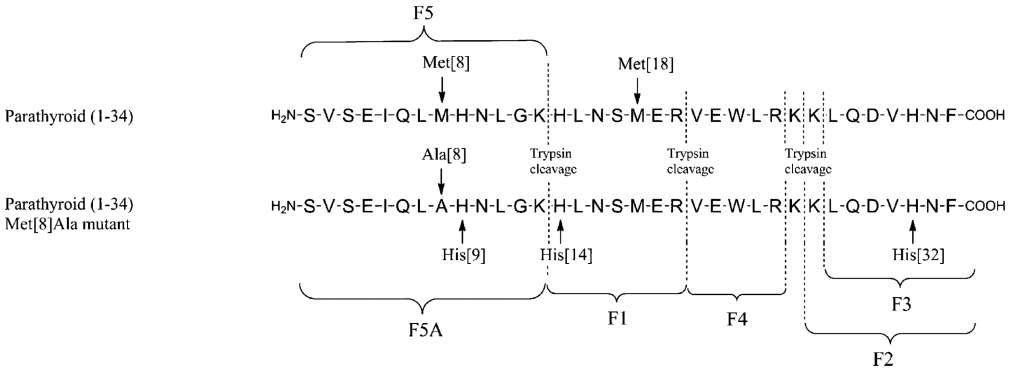

Figure 1.

Representation of the sequences of human parathyroid hormones (PTH(1-34) and PTH(1-34) Met[8]Ala mutant). The dashed lines indicate the digestion sites obtained by means of trypsin in ammonium bicarbonate buffer (50 mM, pH 8). The tryptic fragments are noted as **F1–F5**.

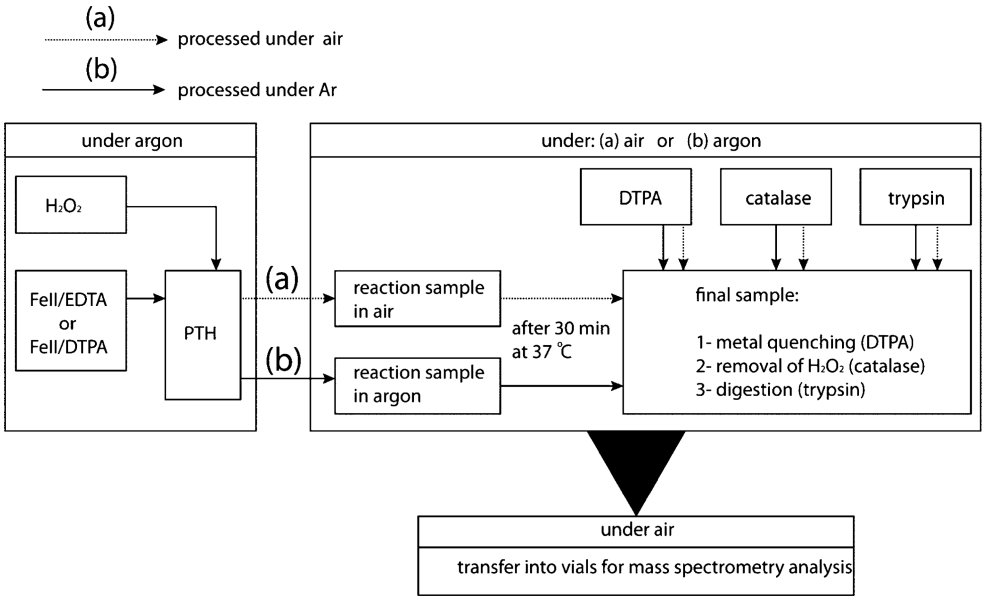

Figure 2.
Schematic representation of the processes used to oxidize and digest PTH(1-34). Pathways a and b describe processes performed under air and Ar, respectively.

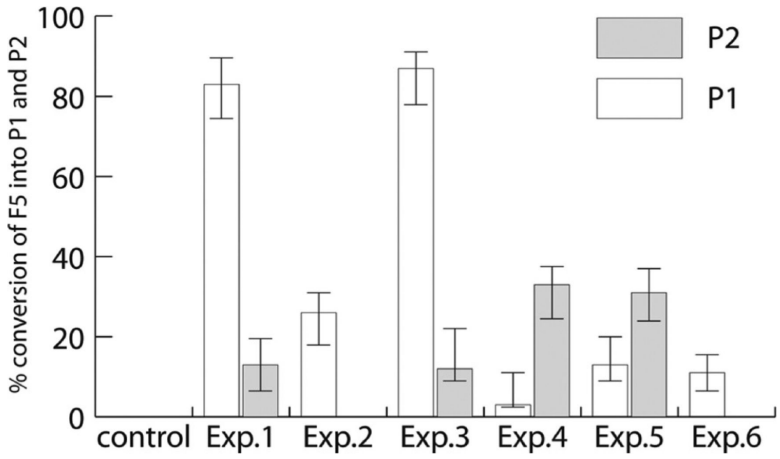

Figure 3.

Percentage of conversion of the tryptic fragment **F5** into products **P1** and **P2** after oxidation of PTH(1-34) under the experimental conditions Exp. 1–6 as described in Section 2.2 and schematized in Figure 2. The bars indicate the lowest and highest ratios of transformation of **F5** into **P1** and **P2** over five replicates.

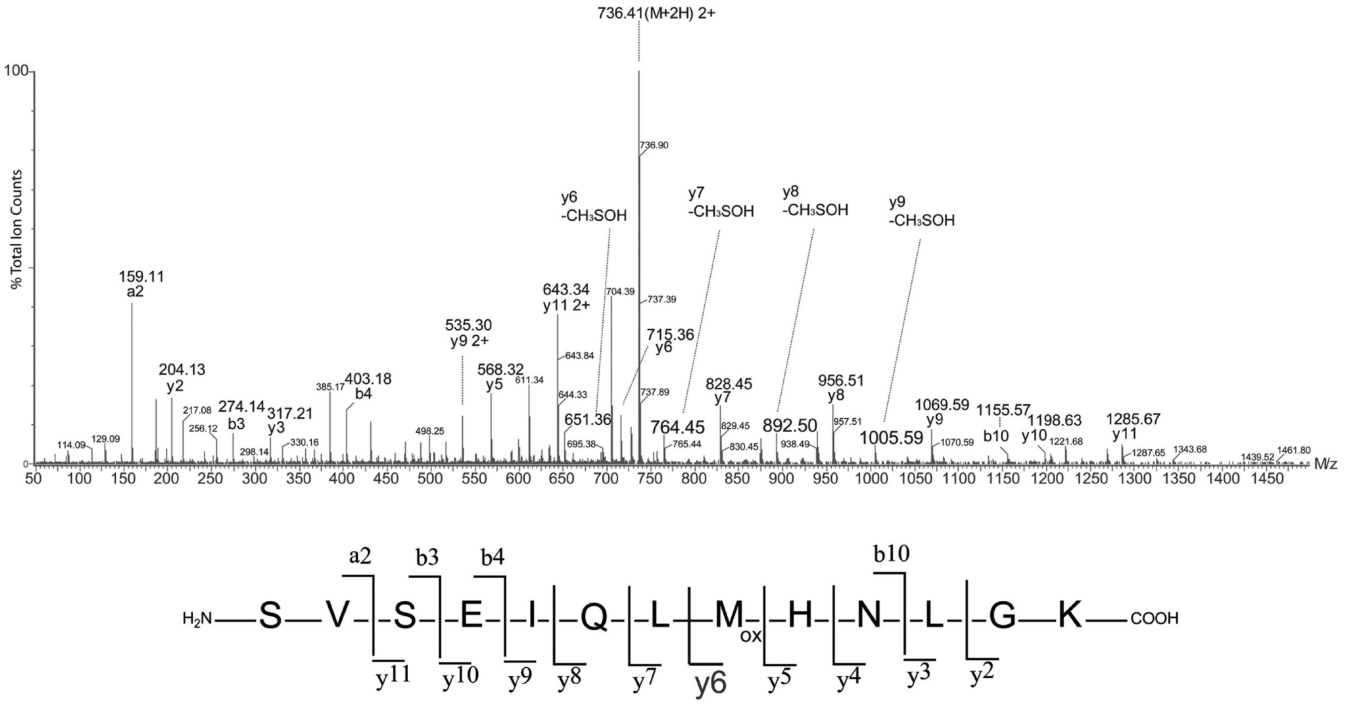

Figure 4.

CID mass spectrum obtained by means of a SYNAPT mass spectrometer of product **P1** (*m/z* 736.4, doubly charged) generated after oxidation of PTH(1-34).

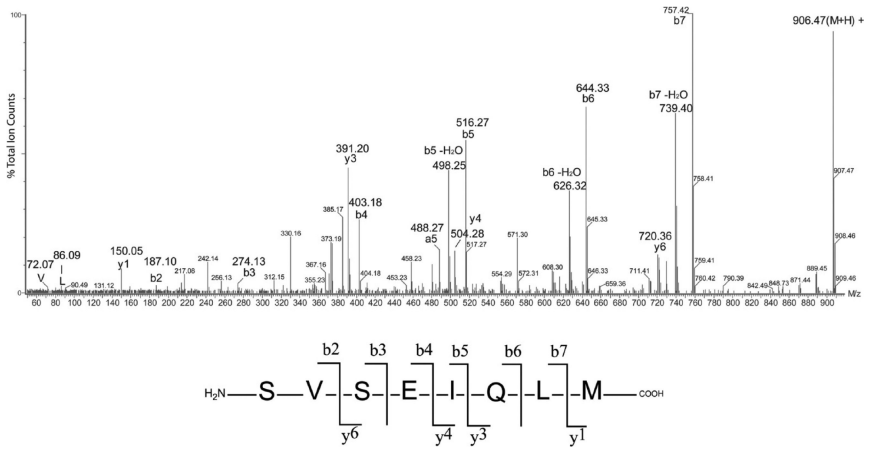

Figure 5.

CID mass spectrum obtained by means of a SYNAPT mass spectrometer of product **P2** (*m/z* 906.4) generated after oxidation of PTH(1-34).

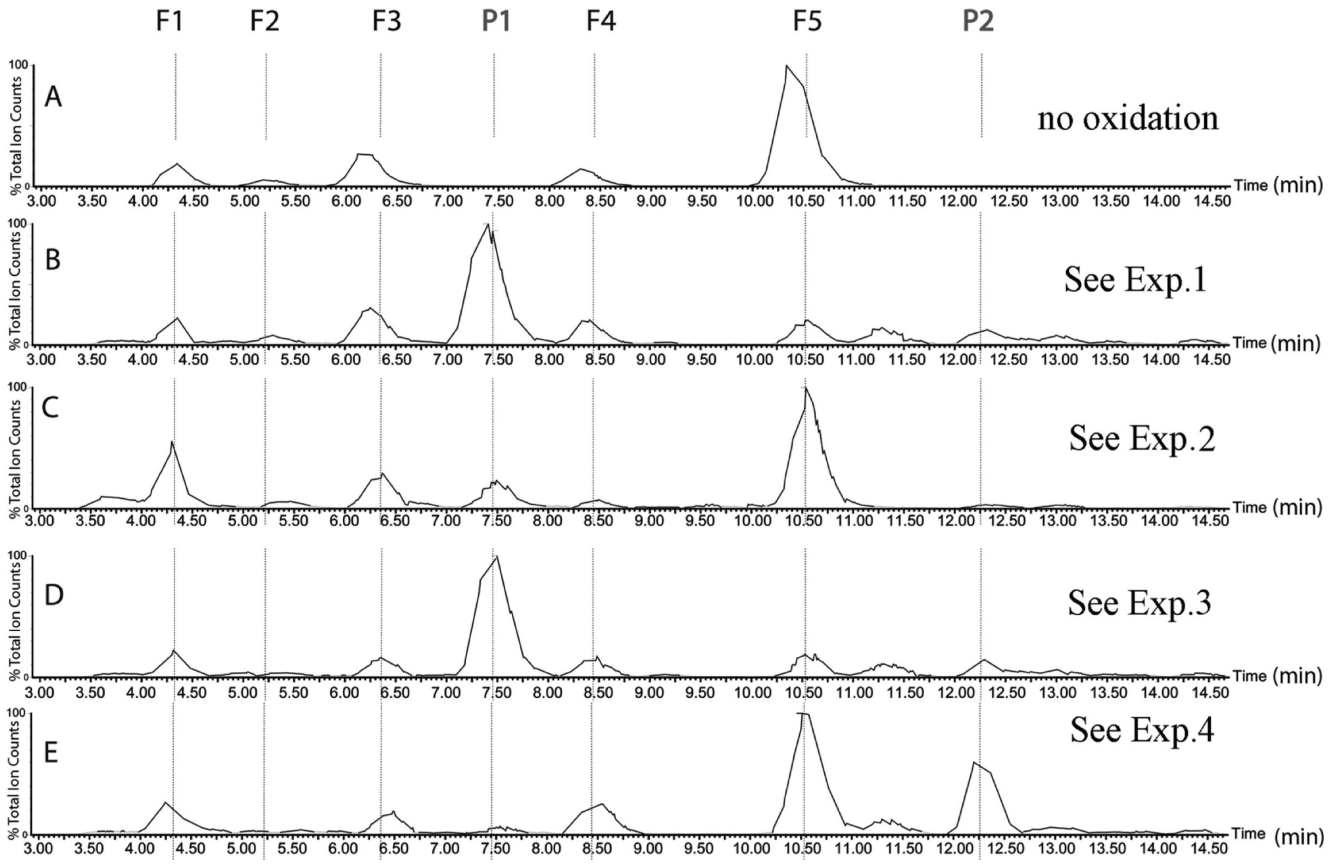

Figure 6.

LC-MS analysis of oxidized PTH(1-34) (24.3 μM) in air: (A) control, no oxidation; (B) oxidation in the presence of $[Fe^{II}/EDTA]^{2-}$ (100 μM) and H_2O_2 (100 μM); DTPA (500 μM) was added to the solution prior to digestion; (C) oxidation in the presence of Fe^{II} and DTPA (100 μM); H_2O_2 (100 μM) and DTPA (500 μM) were added to the solution prior to digestion; (D) oxidation in the presence of $[Fe^{II}/EDTA]^{2-}$ (100 μM) and H_2O_2 (100 μM); (E) oxidation in the presence of $[Fe^{II}/EDTA]^{2-}$ (100 μM); DTPA (500 μM) was added to the solution prior to digestion. In all cases catalase (0.07 μM) was added to the solution prior the digestion.

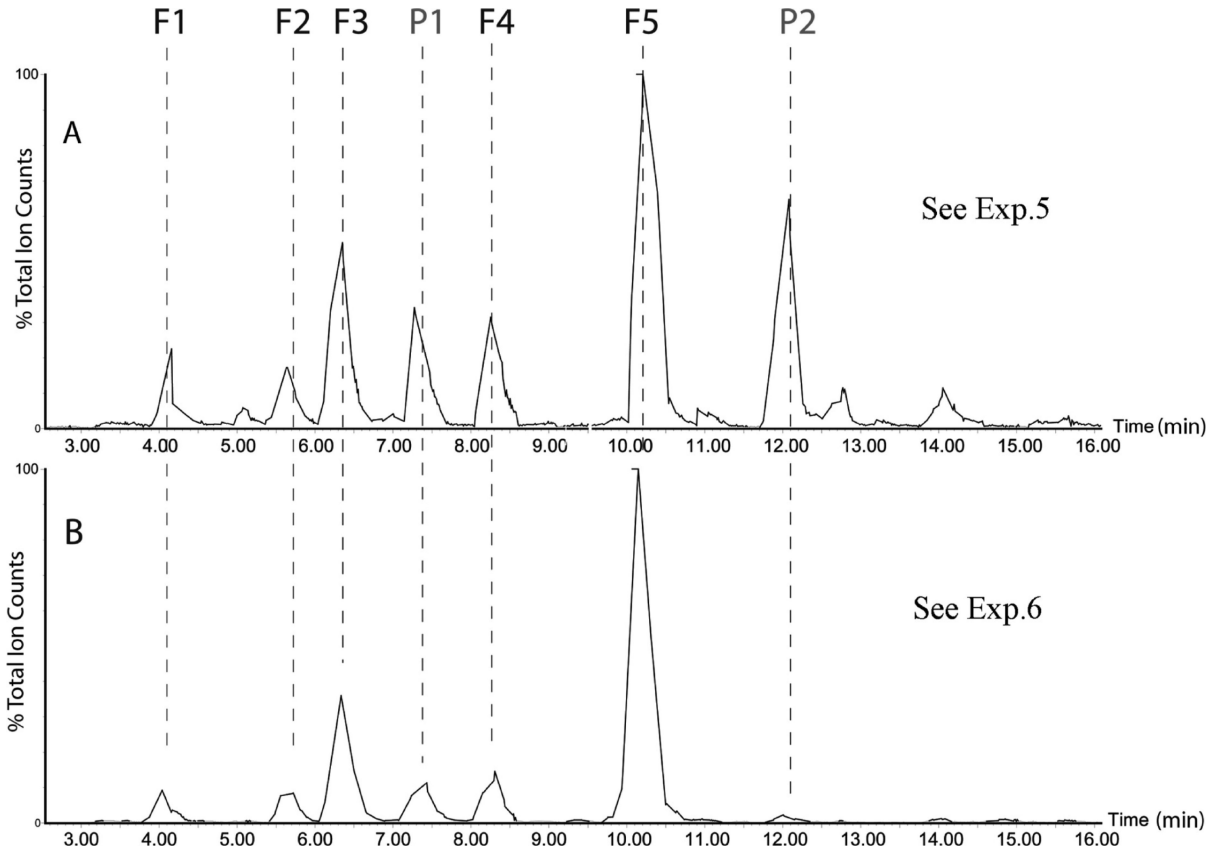

Figure 7.

LC-MS analysis of oxidized PTH(1-34) (24.3 μM) under Ar in the presence of $[Fe^{II}/EDTA]^{2-}$ (100 μM) and H_2O_2 (100 μM): (A) no DTPA was added prior to open the tube to air; (B) DTPA (500 μM) was added in the solution prior exposure of the solution to air and LC-MS analysis. In all the case catalase (0.07 μM) was added under Ar.

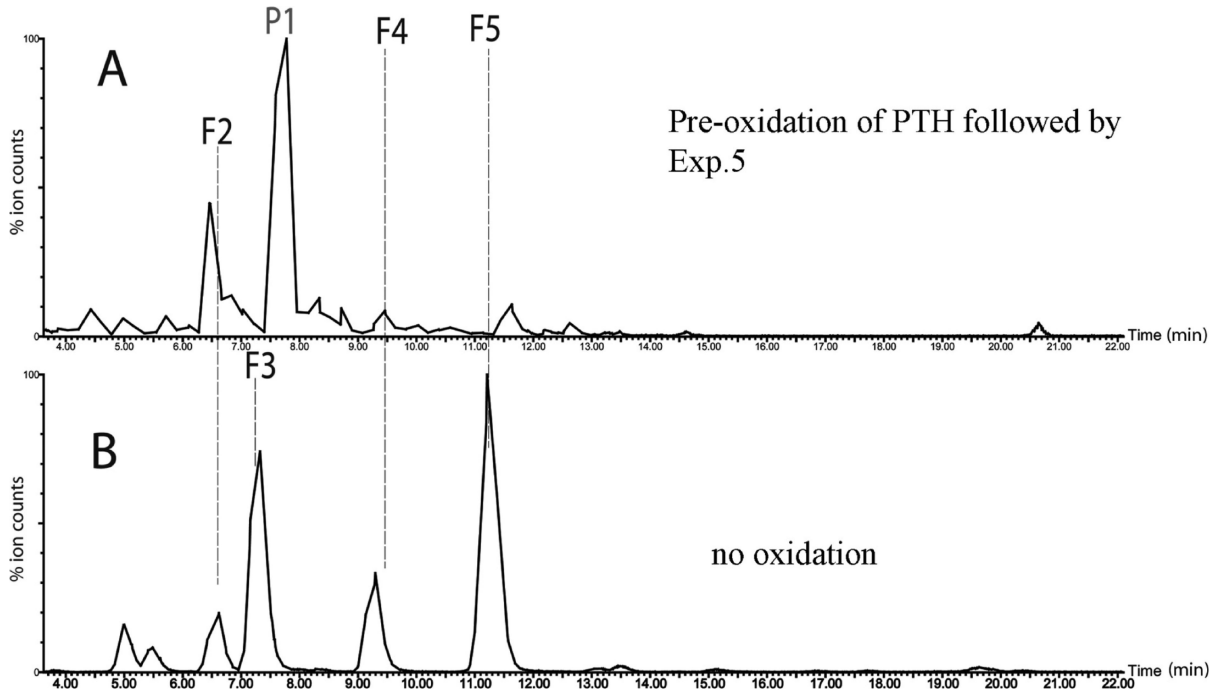

Figure 8.

LC-MS analysis of oxidized PTH(1-34) (24.3 μM): (A) PTH(1-34) preoxidized with H_2O_2 was exposed to $[Fe^{II}/EDTA]^{2-}$ (100 μM) and H_2O_2 (100 μM) under Ar. Catalase (0.07 μM) was added to the solution prior to the digestion, (B) control.

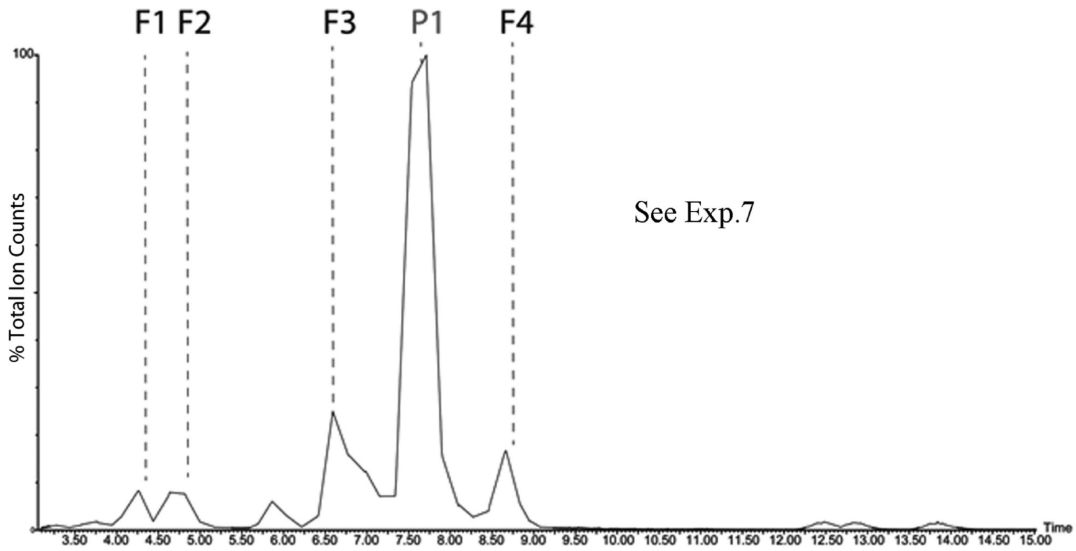

Figure 9.

LC-MS analysis of oxidized PTH(1-34) (24.3 μM) under Ar in the presence of DTPA (100 μM) and H_2O_2 (100 μM). Catalase (0.07 μM) was added under Ar.

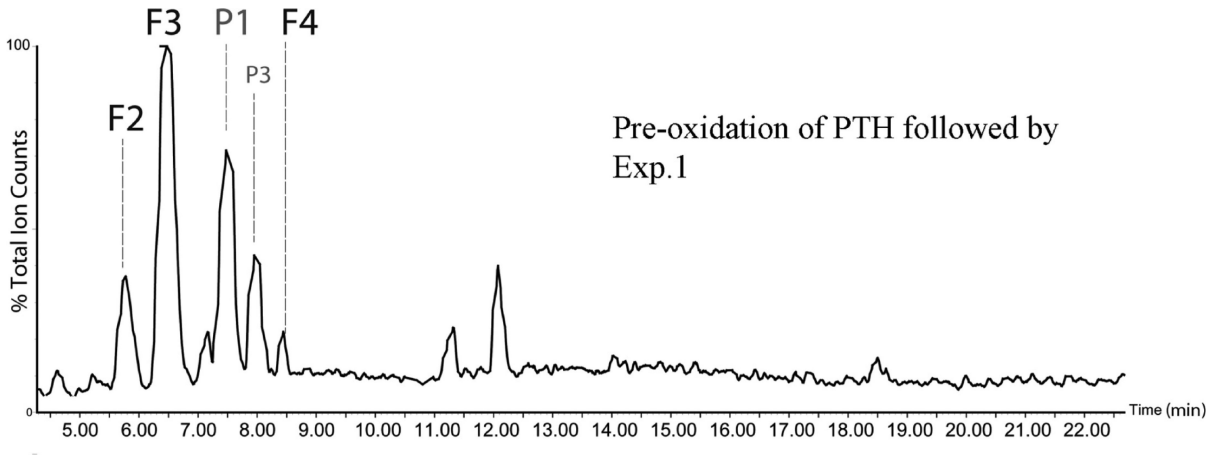

Figure 10.
LC-MS analysis of oxidized PTH(1-34) (24.3 μM) by H_2O_2 and following by Fenton oxidation according to the experimental protocol Exp. 1.

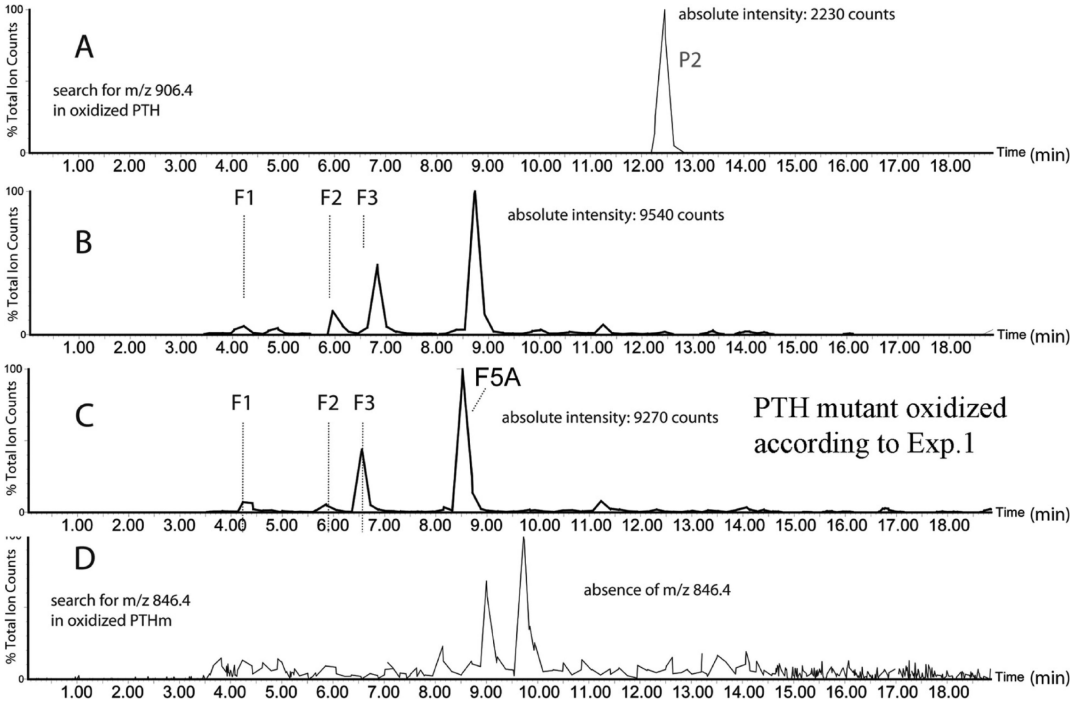

Figure 11.

LC-MS analysis of oxidized PTH(1-34) (24.3 μM) and PTH(1-34) Met[8]Ala (24.6 μM) under air: (A) oxidation of PTH(1-34) in the presence of $[Fe^{II}/EDTA]^{2-}$ (100 μM), H_2O_2 (100 μM); DTPA (500 μM) was added to the solution prior to digestion. The chromatogram highlights product **P2**. (B) Control of nonoxidized PTH(1-34) Met[8]Ala. The MS/MS spectrum of the tryptic fragment **F5A** is presented in Figure S10 (Supporting Information). (C) Oxidation of PTH(1-34) Met[8]Ala in the presence of $[Fe^{II}/EDTA]^{2-}$ (100 μM), H_2O_2 (100 μM); DTPA (500 μM) was added to the solution prior to digestion. (D) oxidation of PTH(1-34) Met[8]Ala in the presence of $[Fe^{II}/EDTA]^{2-}$ (100 μM), H_2O_2 (100 μM), DTPA (500 μM) was added in the solution prior to digestion. Chromatogram D shows the absence of **P2A** (*m/z* 846.4). The absolute intensity for the most abundant species is displayed in each chromatogram.

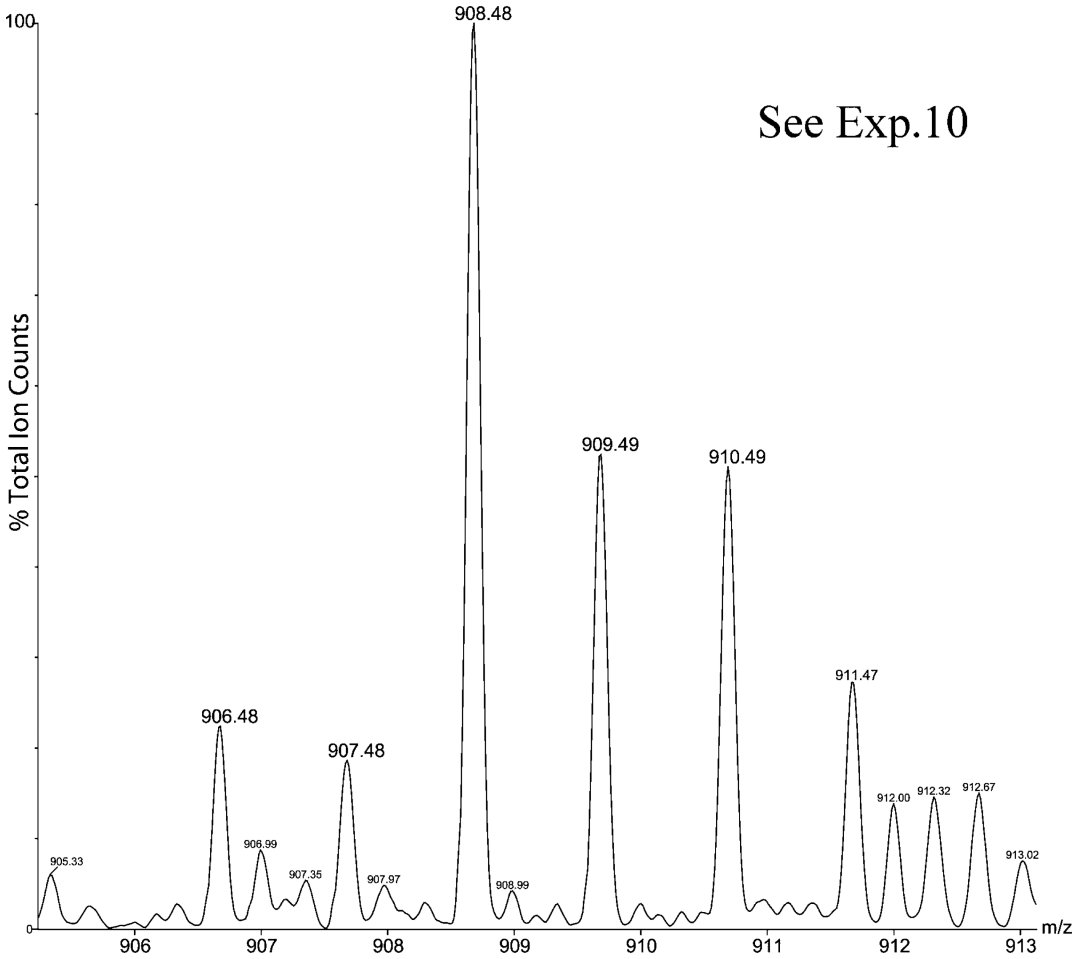

Figure 12.

Oxidation of PTH(1-34) in the presence of H_2O^{18}/H_2O^{16} (80:20, v:v). Mass spectrum in the range of the *m/z* of product **P2** (*m/z* 906.4, when generated in the presence of 100% H_2O^{16}).

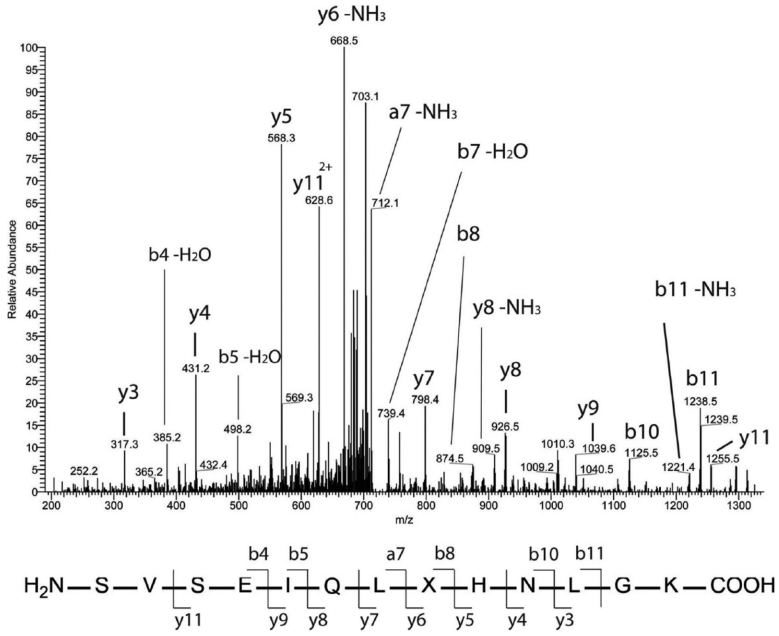

Figure 13.

CID mass spectrum obtained by means of a FT-ICR mass spectrometer of product **P4** (*m/z* 721.4, doubly charged) generated after oxidation of PTH(1-34). X stands for the homocysteine residue.

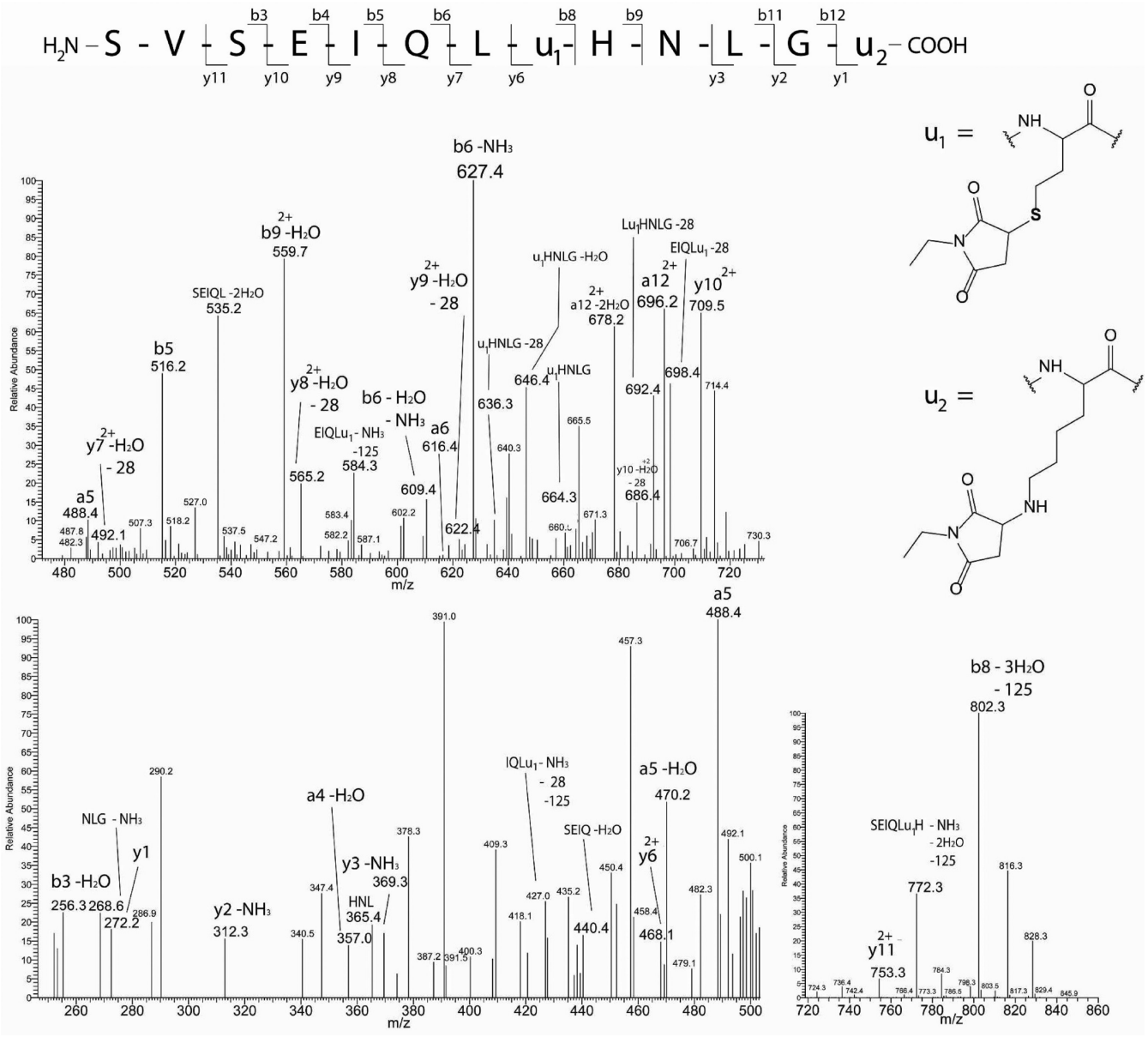

Figure 14.

CID mass spectrum obtained by means of a FT-ICR mass spectrometer of product **P4-NEM** (*m/z* 721.4, doubly charged) generated after oxidation of PTH(1-34). "u_1" and "u_2" stand for the homocysteine and C-terminal lysine residues derivatized with NEM, respectively.

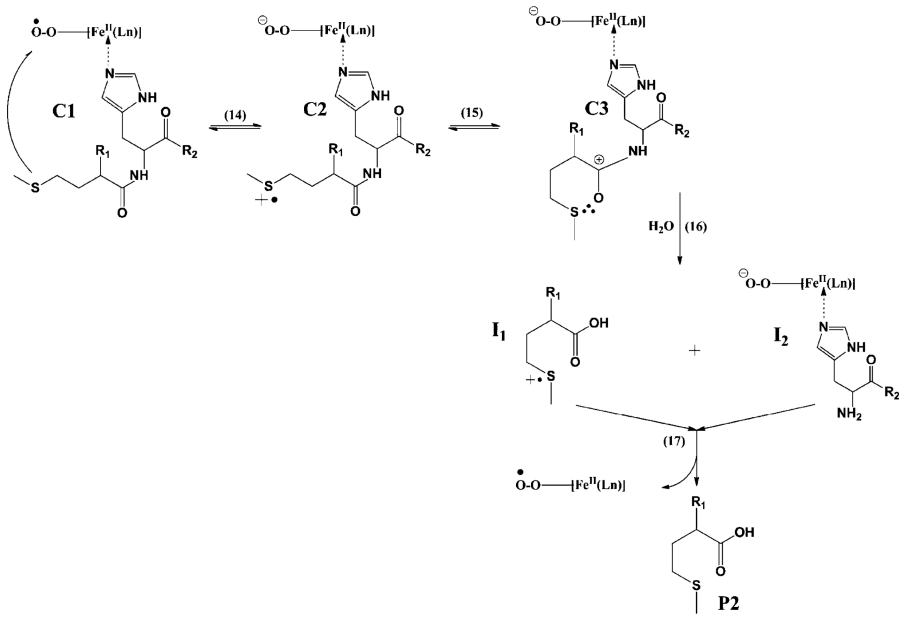

Scheme 1.

Postulated Reaction Mechanism to Rationalize the Formation of P2 during Oxidation of PTH(1-34) by $[Fe^{II}(Ln)]^{m-}$ and Oxygen. (Ln = EDTA, H_2O, or Acetate). R_1 and R_2 Represent the Peptide Sequences SVSEIQL and NLGKHLNSMERVEWLRKKLQDVHNF, Respectively

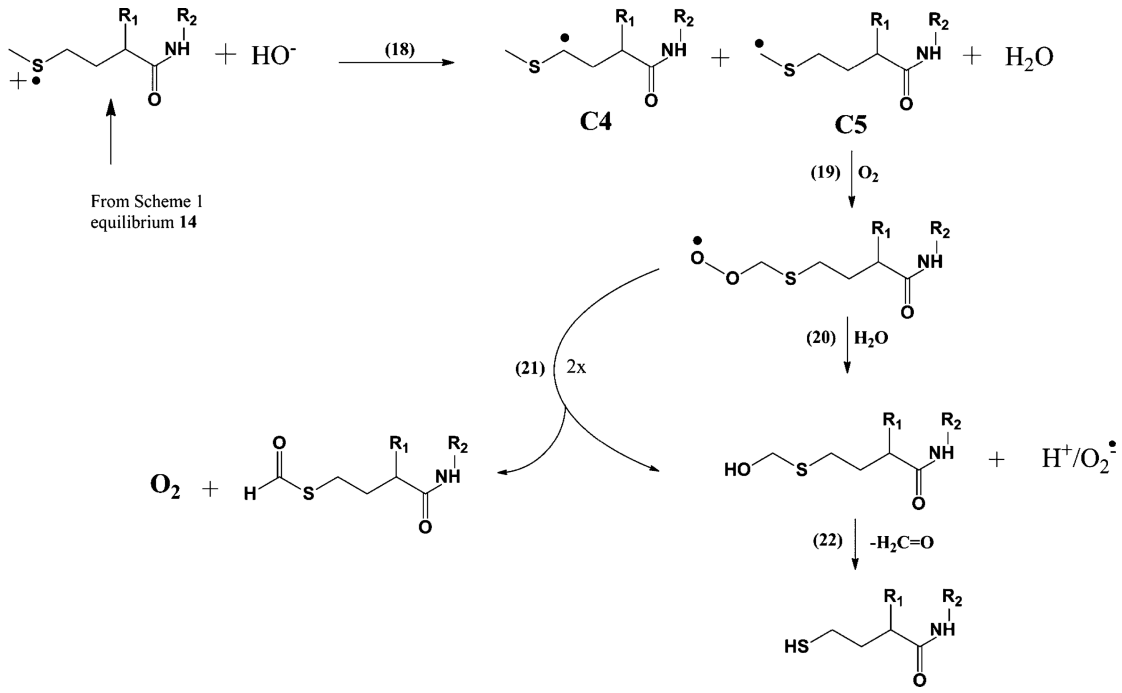

Scheme 2.

Postulated Reaction Mechanism to Rationalize the Transformation of Met[8] into Homocysteine during Oxidation of PTH(1-34). R_1 and R_2 Represent the Peptide Sequences SVSEIQL and HNLGKHLNSMERVEWLRKKLQDVHNF, Respectively

Table 1

Summary of the PTH(1-34) and PTH(1-34) Met[8]Ala Mutant Tryptic Fragments and Products of Oxidation

reference	sequence[a]	MS/MS spectrum
F1	HLNSMER	Figure S1
F2	KLQDVHNF	Figure S2
F3	LQDVHNF	Figure S3
F4	VEWLR	Figure S4
F5	SVSEIQLMHNLGK	Figure S5
F5A	SVSEIQLAHNLGK	Figure S10
P1	SVSEIQLM$_{ox}$HNLGK	Figure 4
P2	SVSEIQLM	Figure 5
P3	SVSEIQLM$_{ox}$H$_{ox}$NLGK	Figure S6
P4	SVSEIQL(Hcys)HNLGK	Figure 13
P2A	SVSEIQLA	not observed

[a] M_{OX} and H_{OX} stand for methionine sulfoxide and 2-oxo-histidine, respectively. In product **P4**, Hcys represents homocysteine.

Table 2

Summary of the Major Results Observed under the Different Conditions of Oxidation

experimental protocol	major observations
Exp. 1	formation of **P1** and **P2**. See Figure 6B
Exp. 2	formation of **P1** only. See Figure 6C
Exp. 3	formation of **P1** and **P2**. See Figure 6
Exp. 4	formation of **P1** with much lower yield than those observed in previous protocols. Increase of the yield of **P2**. See Figure 6E
Exp. 5	formation of **P1** and **P2**. See Figure 7A
Exp. 6	formation of **P1** only. See Figure 7B
Exp. 7	complete oxidation of Met[8] into MetSO (**P1**). **P2** is not formed. See Figure 8A
Exp. 8	formation of **P1** only
Exp. 9	formation of **P1** with a lower yield than those observed in previous protocols. **P2** is observed with a yield similar to that calculated in Exp. 1 and 3
Exp. 10	(1) Mass spectrometry analysis of full PTH (no digestion). (2) Fenton oxidation run in the presence of H_2O^{18}. Incorporation of O^{18} is observed in product **P2**. See Figure 12
Exp. 1 with PTH mutant (Met[8] was replaced by Ala[8])	absence of the hydrolytic cleavage between Ala[8] and His[9]. See Figure 11D
Exp. 1 and excess of exogenous Met	formation of **P2** is prevented
Preoxidation of Met residues to MetSO and His to 2-oxo-histidine prior to apply the experimental protocol Exp. 1	formation of **P2** is prevented